Molecular mechanisms of DNA replication across UV-induced DNA lesions and novel approaches to suppress UV mutagenesis

Lavanya Samraj

A thesis

submitted in partial fulfillment of the

requirements for the degree of

Master of Science

University of Washington

2017

Supervisory Committee:

Paul Nghiem (Chair)

Masaoki Kawasumi

Richard Presland

Program Authorized to Offer Degree:

Oral Biology

University of Washington

Abstract

Molecular mechanisms of DNA replication across UV-induced DNA lesions and novel approaches to suppress UV mutagenesis

Lavanya Samraj

Chair of the Supervisory Committee:

Professor. Paul Nghiem

Division of Dermatology

Skin cancer is the most prevalent cancer in humans, with an annual incidence of 5.4 million in the U.S. Ultra Violet (UV) irradiation generates DNA lesions that are potentially mutagenic, and accumulation of mutations eventually leads to skin cancers. UV irradiation generates two major types of DNA lesions: cyclobutane pyrimidine dimers (CPDs) and 6-4 photoproducts (6-4PPs) that can cause replication stalling. To cope with the replication-blocking lesions, cells employ a specialized damage tolerance process known as translesion synthesis (TLS), that is potentially mutagenic. The two types of UV lesions are structurally distinct and are bypassed by DNA polymerases differently. Importantly, 6-4PP is more mutagenic than CPD. A major cell cycle checkpoint kinase known as Ataxia-Telangiectasia Mutated and RAD3-related (ATR) is

activated after UV. ATR is critical for the cells to survive UV damage, but could also increase the risk of mutations by increasing the survival of DNA-damaged cells. ATR inhibition augments the apoptosis of UV-damaged cells, thereby suppressing UV carcinogenesis. However, whether ATR promotes mutations in UV-damaged cells remains unclear. It is of interest to investigate whether ATR inhibition reduces mutations in cells surviving UV damage. We hypothesized that ATR is required for promoting error-prone TLS. TLS bypass of 6-4PP lesions increases mutations leading to UV-induced carcinogenesis. In this study, we analyzed the effect of ATR inhibition in TLS activity at 6-4PP lesions. We measured the percentage of unbypassed 6-4PP lesions surrounded by single-stranded DNA by using a lesion-specific antibody using flow cytometry. If ATR is facilitating 6-4PP bypass, ATR inhibition is expected to increase the number of unbypassed 6-4PP lesions. Our results showed that the percentage of unbypassed 6-4PP lesions were increased when ATR is inhibited by pharmacologic inhibition (VE-821/caffeine) compared to cells without ATR inhibition. This implies that ATR is likely involved in 6-4PP lesion bypass. The unbypassed 6-4PP lesions might eventually get repaired or progress into double-strand DNA breaks leading to apoptosis. Therefore, blocking error-prone TLS activity by ATR inhibition using VE-821 or caffeine might reduce mutation incorporation and thereby suppression of UV carcinogenesis.

TABLE OF CONTENTS

APPROVAL PAGE.....1

DECLARATION.....2

ABSTRACT.....3

TABLE OF CONTENTS.....5

CHAPTER ONE: GENERAL INTRODUCTION AND BACKGROUND.....6

CHAPTER TWO: MATERIALS AND METHODS.....23

CHAPTER THREE: RESULTS.....31

CHAPTER FOUR: DISCUSSION.....45

CHAPTER FIVE: SUMMARY AND FUTURE DIRECTIONS.....50

BIBLIOGRAPHY.....51

ACKNOWLEDGMENTS.....55

CHAPTER ONE: GENERAL INTRODUCTION AND BACKGROUND

1.1 Nonmelanoma skin cancer

Nonmelanoma skin cancer is the most prevalent cancer in the U.S. with an annual incidence of 5.4 million[1]. Ultraviolet (UV) irradiation is the major causal factor in nonmelanoma skin cancers[2]. UV radiation generates DNA lesions, which contribute to mutations and eventually leads to skin cancer.

1.2 UV lesions

1.2.1 UV irradiation

Ultra Violet (UV) radiation has been proven to be a major carcinogen for both melanoma and non-melanoma skin cancers. UV radiation comprises a spectrum of different wave lengths with distinct physical properties and biological effects[3]. Based on wavelength, UV radiation is classified into UV-A (320–400 nm), UV-B (280–320 nm) and UV-C (100–280 nm). All UV-C and most of UV-B radiation (90%) are absorbed by the atmosphere.

1.2.2 Two major types of UV-B lesions: CPD and 6-4PP

UV-A radiation induces oxidative damage to DNA and this type of lesion has been linked to the carcinogenesis of melanoma[3,4]. UV-B (280–320 nm) is the most relevant wavelengths of UV in the carcinogenesis of non-melanoma skin cancers[5]. UV-B generates two major types of lesions: cyclobutane pyrimidine dimers (CPDs) and pyrimidine (6-4) pyrimidone photoproducts [(6-4) photoproducts; 6-4PP]. These two types of lesions differ in the chemical bond between the pyrimidine bases. CPD is formed by a ring structure between C5 and C6 of the adjacent pyrimidine

bases (e.g., T=T, T=C), whereas a 6-4PP lesion is formed by non-cyclical bond between C6 (5' end) and C4 (3' end) of pyrimidine bases (Figure 1.1a).

A 6-4PP lesion causes more DNA helical distortion (44º bending of DNA) than a CPD lesion (9º bending of DNA)[6,7] (Figure 1.1b). Both types of lesions can only occur between adjacent pyrimidine bases, and such sites are known as 'hotspots' of UV-induced mutations[8].

CPD lesions are the most abundant UV-B induced lesions. Mammalian cells that received 1 kJ/m^2 of UV-B radiation (equivalent to 3.5-4 h of sun exposure at mid-day in summer) formed CPD lesions at the rate of 0.22 per kbp of DNA and 6-4PP lesions are formed at the rate of 0.024 per kbp of DNA[9]. Another study that used 300 J/m^2 of UV-B radiation, showed five-fold more CPD (55 lesions per 10^6 DNA pairs) than 6-4PP lesions (12 lesions per 10^6 DNA pairs)[10].

Repair of 6-4PP lesions reduced UV-induced apoptosis significantly compared to repair of CPD lesions alone, indicating 6-4PP is a potent inducer of apoptosis compared to CPD[10]. These two types of lesions contribute differently to UV mutagenesis[11].

1.3 UV-induced DNA lesions: Repair and damage tolerance mechanisms

1.3 Repair of UV-induced DNA lesions by Nucleotide Excision Repair (NER)

Most UV-induced DNA lesions are removed by nucleotide excision repair (NER), a DNA repair mechanism that can repair UV-induced DNA lesions in an error-free manner. NER has two subpathways: global genome NER (GG-NER) and transcription-coupled NER (TC-NER). The GG-NER subpathway is activated in the entire genome at sites of helix distortion irrespective of transcription, whereas TC-NER is activated only when RNA polymerase II (RNA Pol II) is stalled during transcription[12]. The two subpathways differ only in the initial damage recognition step, but share common repair mechanisms.

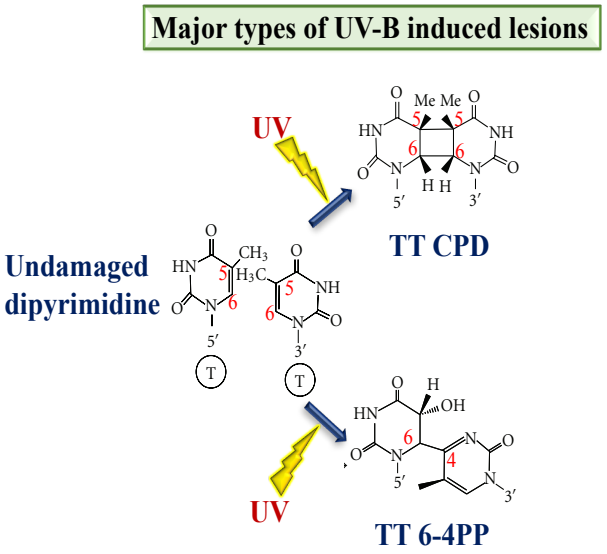

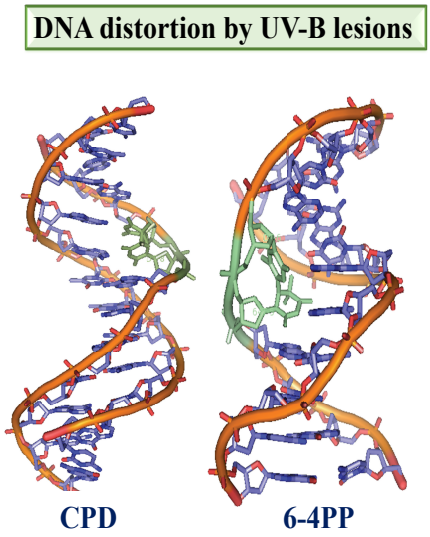

Figure 1.1a **Figure 1.1b**

Figure 1.1a. UV-B generates two major types of lesions.

CPD is formed by ring structure between C5 and C6 of adjacent pyrimidines, while 6-4PP is formed by non-cyclical bond between C6 and C4 of pyrimidine bases.

Figure 1.1b. 6-4PP causes more helical distortion compared to CPD.

6-4PP (green color) causes severe helical distortion (~44º bending) compared to CPD (green color) (9º bending).

Adapted from Rastogi et al. J Nucleic Acids. 2010 Dec 16;2010:592980.

Xeroderma Pigmentosum-C (XP-C) protein together with RAD23B is the main damage sensor in GG-NER. In TC-NER, Cockayne syndrome (CSB) protein binds with RNA Pol II, when there is polymerase stalling at a lesion. The initial recognition step is followed by damage verification step, dual incision for removal of the lesion, then gap-filling.

XP-C binding enables recruitment of another factor TFIIH (transcription initiation factor IIH) for lesion verification. After this step, dual incision by endonucleases XPF-ERCC1 and XPG removes the lesion. XPA is another important molecule that coordinates the binding of TFIIH and orients the endonucleases accurately at the lesion site. Final DNA gap-filling synthesis and ligation are executed by the replication proteins Proliferating Cell Nuclear Antigen (PCNA), replicative polymerases polymerase delta (Pol δ), polymerase epsilon (Pol ε) or polymerase kappa (Pol κ), and DNA ligase-1 or XRCC1–DNA ligase 3.

6-4PP lesions have a half-life of 2-2.5 hours and are almost completely removed by 24 hours. In contrast, 51-76 % of CPD lesions remain after 24 hours[9]. The slow corrective mechanism probably relates to the fact that CPD lesions form poor substrates for XP-C and the recognition process requires an auxiliary protein, the UV–DDB (ultraviolet radiation–DNA damage binding protein) complex[12].

DNA repair disorders in humans such as xeroderma pigmentosum (XP), Cockayne syndrome (CS), and trichothiodystrophy (TTD) indicate the significance of NER repair[13]. XP is an autosomal recessive disorder characterized by defective NER pathway, leading to extreme UV sensitivity. XP belongs to heterogenous group of genetically different diseases [XP-A to XP-G and XP-Variant (XP-V)], based on the respective defects in genes that encode proteins involved in NER. XP-V has intact NER, but is defective in a polymerase (Pol eta) that is important for damage tolerance mechanisms for unrepaired lesions. This indicates that both repair and damage tolerance

mechanisms are equally important for the cells to survive UV damage. Defective repair/tolerance of UV lesions make these patients hypersensitive to UV-induced DNA lesions and prone to skin cancers. Cockayne syndrome is related to mutations mainly in CSA and CSB genes leading to defective TC-NER subpathway. These patients have severe developmental abnormalities and premature ageing leading to reduced lifespan. Cockayne syndrome patients generally do not survive long enough to develop skin cancer[13]. There is a combined type with XP (CS/XP), in which there are reports of early childhood skin cancer[13].

1.4 Damage tolerance mechanisms of UV-induced DNA lesions

Though NER efficiently repairs UV lesions, there are other damage tolerance mechanisms that occur when the lesion is not repaired before the cell enters S phase. Replicative polymerases such as Pol delta (δ) and Pol epsilon (ε) normally synthesize DNA across undamaged DNA. These replicative polymerases are predominantly B-family polymerases and their error-rate is in the range of 10^{-6} to 10^{-8} indicating the high fidelity of these polymerases[14].

When cells enter S phase of the cell cycle before complete removal of these lesions, replicative DNA polymerases cannot continue DNA synthesis across these highly DNA-distorting lesions, leading to replication fork stalling (Figure 1.2). UV irradiation activates checkpoint kinases and damage tolerance mechanisms to facilitate DNA replication that cope with these DNA lesions. DNA damage tolerance mechanisms include homologous recombination and translesion synthesis[15].

1.5 Translesion synthesis

Translesion synthesis is an error-prone process that plays an important role in UV mutagenesis. Translesion synthesis (TLS) is a mechanism that can synthesize DNA across damaged or distorted DNA lesions. The lesions are bypassed by specialized DNA polymerases known as TLS polymerases that incorporate nucleotides directly opposite the lesions (Figure 1.2).

In eukaryotes, TLS polymerases were first identified in the yeast Saccharomyces cerevisiae, which has three different translesion synthesis polymerases, i.e. Reversionless 1 (Rev1), Pol eta (η) and Pol zeta (ζ). Polymerase iota (ι) and kappa (κ) are additional TLS polymerases in mammals. Rev1, Pol eta, Pol iota and Pol kappa belong to Y-family polymerases and Pol zeta is part of the B-family of DNA polymerases[16]. TLS polymerases differ structurally from replicative polymerases, in particular, they have catalytic sites that can accommodate bulky chemical groups adducted to template bases[17]. TLS polymerases are low-fidelity polymerases with error rates ranging from 10^{-3} to 10^{-1} due to lack of a proof-reading exonuclease[14,15]. TLS polymerases bypass the lesion with frequent misincorporation of nucleotides, resulting in mutations[18-20]. Thus, elucidating TLS mechanisms is important to the goal of suppressing UV mutagenesis.

1.6 TLS mechanisms differ in CPD and 6-4PP

TLS occurs when the replicative polymerase stalls at a UV lesion. Proliferating cell nuclear antigen (PCNA) also known as eukaryotic DNA sliding clamp is a major regulator involved in the recruitment of proteins to sites of DNA replication[21]. Replication stalling at DNA lesions causes post-translation modifications in PCNA. Mono-ubiquitination of PCNA (lysine 164, K164) is a key event in TLS, as it enables the 'polymerase switch' from replicative polymerase to TLS polymerase. Once the TLS polymerase has incorporated the required number of nucleotides, the

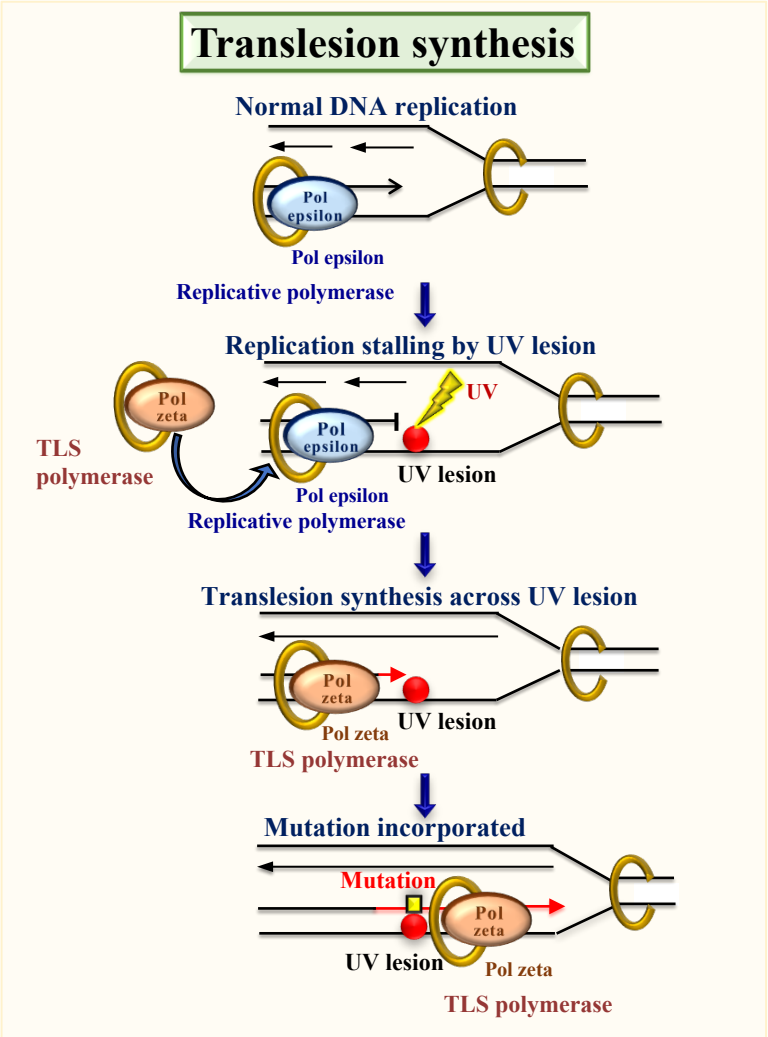

Figure 1.2. Translesion synthesis across UV lesions.

During normal DNA replication, a replicative polymerase (Pol epsilon) synthesizes DNA with high fidelity. UV generates DNA lesions that stall replication because the replicative polymerase is not able to bypass a UV lesion. A translesion synthesis (TLS) polymerase (Pol zeta) can synthesize DNA opposite the lesion, but it frequently incorporates mutations.

polymerase dissociates from DNA due to their poor processivity[22]. Also studies have shown deubiquitination of PCNA to be responsible for TLS polymerase dissociation[22]. After the dissociation of TLS polymerase, the replicative polymerase binds to PCNA, to continue DNA replication.

The mechanisms of TLS differ between CPD and 6-4PP lesions. CPD lesions are predominantly bypassed by a co-replication model, in which a single polymerase (e.g., Pol eta) completely bypasses the lesion and the replication proceeds with replicative polymerase[23]. TLS of a helix-distorting or bulky nucleotide lesion, that cannot be bypassed by a single TLS polymerase, may involve multiple specialized DNA polymerases that act in a consecutive fashion in mammalian cells. 6-4PP is bypassed by a gap-filling mechanism[16] (Figure 1.3). The two-polymerase or gap-filling model involves one inserter polymerase which is usually Pol eta or Pol iota, and extender polymerase which is usually Pol zeta[24].

In the gap-filling model of TLS, when there is replication block, there is a replication restart a few bases downstream of the lesion by repriming (Figure 1.3). PrimPol has been shown to be an important polymerase in this repriming process on the leading strand of DNA[25]. This repriming leaves behind a single-stranded DNA with an unbypassed UV lesion[16,26]. This gap is later filled by combination of extender TLS polymerase (Pol zeta) and replicative polymerase in late S phase or G2 phase of cell cycle.

1.7 Mutagenicity of UV-B lesions

CPD lesions are usually bypassed by Pol eta, whereas 6-4PP bypass is usually carried out by Pol zeta. Pol eta-mediated CPD bypass is error-free, whereas Pol zeta frequently misincorporates

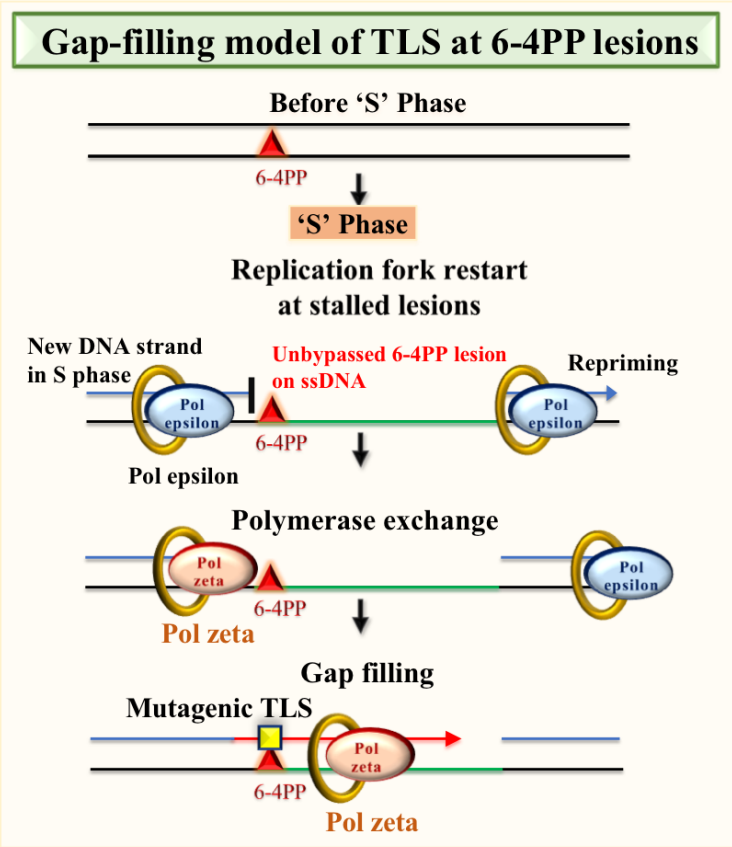

Figure 1.3. Speculative model for translesion synthesis at post-replicative gaps (6-4PP lesions).

In gap-filling model of TLS, when there is replication block, there is replication restart few bases downstream the lesion by repriming. The new DNA strand is denoted by top line in S phase. The existing DNA strand is left with unbypassed 6-4PP lesion surrounded by single-stranded DNA (ssDNA). This ssDNA gap is later filled by recruitment of combination of polymerases, replacing replicative polymerase (polymerase exchange). Pol zeta is the predominant polymerase that bypasses 6-4PP lesions and incorporate mutations by gap-filling mechanism.

Adaped from Jansen et al. DNA Repair. 2015;29:56–64.

nucleotides opposite 6-4PP lesions[15,27,28]. Therefore, TLS mechanisms can be error-free or error-prone depending on the lesion and the polymerase that is recruited to the lesion.

The significance of error-free TLS by Pol eta is evident in XP-V patients who have defective Pol eta activity. When Pol eta is absent, CPD lesions are bypassed by error-prone polymerases such as Pol zeta and Pol iota leading to increased susceptibility to UV mutagenesis[17].

TLS across 6-4PP lesions is more mutagenic than that across CPD lesions[29]. Depletion of Pol zeta decreases UV-induced mutation frequency up to 4-5 fold compared to wild-type cells[30]. Despite the fast repair rate, 6-4PP lesions are more mutagenic probably due to the error-prone TLS activity. It is therefore important to know the significance of each TLS polymerase for better understanding of UV mutagenesis.

1.8 The significance of error-prone TLS by Pol zeta in 6-4PP

Since 6-4PP lesions are more mutagenic compared to CPD lesions[11], it is important to understand the TLS bypass mechanisms at 6-4PP because there is the possibility of reducing mutations by targeting the specific TLS polymerase. Pol zeta has been shown to be the major polymerase involved in 6-4PP bypass.

Polymerase zeta is a heterodimer containing the Rev3 catalytic subunit and the Rev7 regulatory subunit. The Rev genes (Reversionless) Rev1, Rev3 and Rev7 were first demonstrated to be involved in mutagenic replication of damaged DNA in S. cerevisiae [24]. The mammalian gene counter part of Rev3, known as Rev3-like (REV3L) encodes a polypeptide of ~353 kDa, twice as large as the catalytic subunit of yeast Pol zeta. Endogenous REV3L expression is very low in mammalian cells[31].

Rev3 is dispensable in yeast, whereas deletion of REV3L (Rev3-like) cause embryonic lethality in the mouse indicating the essential role of REV3L. Lange et al. showed an absence of UV-induced tumors when there is deletion of REV3L in murine skin[32]. Pol zeta defective skin showed increased sensitivity to UV radiation leading to increased cell death. This study suggested that temporary inhibition of Pol zeta when there is UV-induced DNA damage could be protective against UV carcinogenesis.

REV7, the smaller subunit of Pol zeta, has been shown to interact with REV3L and REV1. The molecular weight of human REV7 protein was predicted to be 24 kDa. Human REV1 cDNA encodes a 1251 amino acid protein with a predicted molecular weight of 138 kDa.

REV1 has a dCMP transferase activity that enables the insertion of Cytosine across a template Guanine and acts as an inserter polymerase in TLS. REV1 interacts with monoubiquitinated PCNA and promotes the recruitment of Pol zeta to 6-4PP sites[16]. REV1 acts as a scaffolding protein facilitating the TLS activity at 6-4PP involving multiple polymerases.

1.9 Mutagenicity of Pol zeta

Pol zeta is important for maintaining genome integrity when there is DNA damage, and promoting cell survival, but Pol zeta also increases mutations[24]. Pol zeta is responsible for 96% of UV-induced mutations and half of spontaneous mutations. The single base substitution error rate for Pol zeta has been shown to be 10^{-3}. Pol zeta is prone to generate C-G to G-C transversions in vivo. Pol zeta showed multiple single base substitutions in short patches of 6-10 nucleotides. It is possible that Pol zeta generates its own mismatches and extends them contributing to its high mutagenicity[24].

1.10 The role of ATR in UV lesions

When there is UV-induced DNA damage, cells activate DNA damage response pathways that trigger number of events controlling cell proliferation and repair. The major regulators of the DNA-damage response are the phosphoinositide 3-kinase (PI3K)-related protein kinases (PIKKs), including ataxia-telangiectasia mutated (ATM) and ATM and RAD3-related (ATR)[33]. Both kinases phosphorylate serine or threonine residues on target substrates once they are activated. Both ATM and ATR share several downstream target proteins, and differ mainly in the activation mechanism. ATM is activated mainly by double-strand breaks (DSBs) whereas ATR is activated by replication stalling.

ATR is a pivotal kinase that senses replication stress and regulates the cell cycle to help cells survive DNA damage[33]. Replication fork stalling caused by UV lesions activates the ATR pathway (Figure 1.4). When there is replication stalling, it leads to long stretches of single stranded DNA bound by replication protein A (RPA). RPA interacts with ATR-recruiting protein (ATRIP) and recruits ATR to sites of DNA damage. ATR activation requires several other proteins that form part of the ATR-activation complex. This includes Rad17-replication factor C complex, which loads the PCNA-like 9-1-1 clamp (Rad9-Hus1-Rad1) onto primer-template junctions. The 9-1-1 complex then recruits an important activator, topoisomerase-binding protein-1 (ToPBP1), to ATR[33]. The ATR activation domain of TopBP1 interacts and activates the ATR-ATRIP complex[33]. The ATR kinase activates downstream targets, including Chk1, to induce cell cycle arrest and promote DNA repair. ATR activates Chk1 by phosphorylating Ser345 residue. Chk1 activation causes stabilization of replication forks, thus preventing formation of double-strand DNA breaks (Figure 1.4).

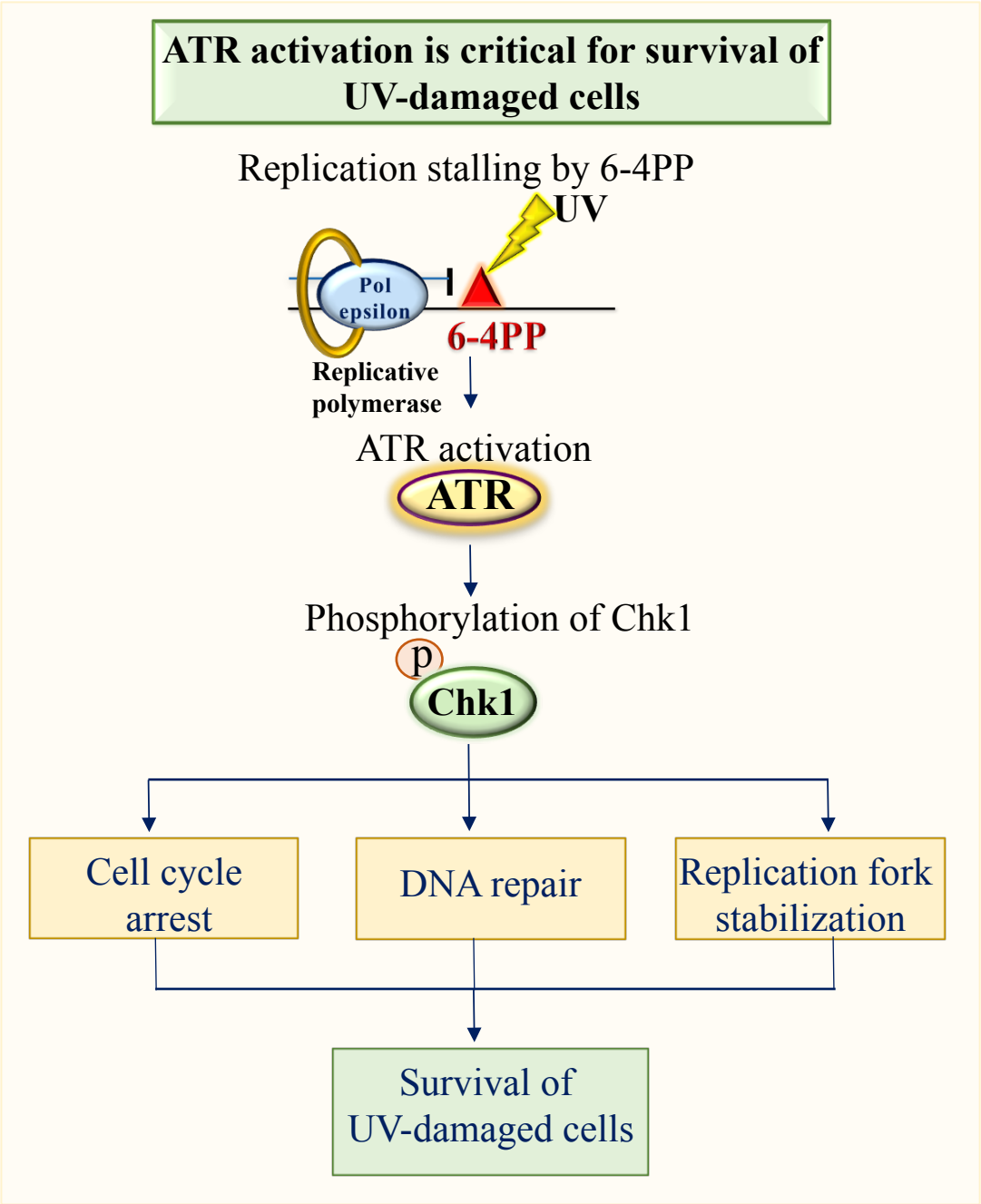

Figure 1.4. ATR activation at UV lesions is important for survival of UV damaged cells. Stalled replication fork at 6-4PP recruits a pivotal cell cycle check point kinase ATR, leading to formation of ATR activation complex including several other proteins. ATR activation causes phosphorylation of multiple downstream targets, mainly phosphorylation of Chk1 ultimately leading to cell cycle arrest, DNA repair, replication fork stabilization. All these events contribute to survival of UV damaged cells.

Inhibition of ATR after DNA damage leads to premature chromatin condensation. This premature entry into mitosis before completion of DNA replication leads to cell death[34]. ATR inhibition augments apoptosis of UV-damaged cells that could become precancerous[35], and thus ATR inhibition may be beneficial to prevent skin cancer development. Indeed, genetic inhibition of ATR suppresses UV carcinogenesis in mice[36].

1.11 Caffeine and skin cancer prevention

Intriguingly, human epidemiological studies have shown that caffeine intake is associated with decreased risk of developing melanoma and nonmelanoma skin cancers[37-39]. The anticancer effect of caffeine has also been documented in other types of cancers[40]. A population-based prospective cohort study showed an inverse correlation between caffeine consumption and incidence of oral and oropharyngeal cancers. Another study that documented pooled-analysis of nine case-control studies based on a total of 5139 cases of cancer of Oral and Oropharyngeal cancers have also shown inverse correlation between caffeine consumption and an incidence of oral and oropharyngeal cancers [41].

Because caffeine is a nonspecific inhibitor of the ATR kinase[42], it has been proposed that augmented apoptosis of UV-damaged cells via ATR inhibition is a likely mechanism by which caffeine prevents skin cancer. However, there might be additional mechanisms underlying skin cancer prevention by ATR inhibition or caffeine: ATR inhibition may block the mutation incorporation process that occurs at UV lesions.

In our preliminary studies, topical application of caffeine on mouse skin immediately after UV irradiation reduced incidence of skin cancers compared to application of caffeine weeks after

irradiation (delayed application of caffeine). This indicates that the cancer preventive effect of caffeine is highly associated with the time of caffeine application post-UV irradiation.

We hypothesize that immediate ATR inhibition after UV radiation may block error-prone translesion synthesis. Importantly, we recently found that ATR is activated by 6-4PP lesions that are highly mutagenic, but not by CPD lesions (manuscript in revision). We hypothesize that ATR activation at 6-4PP lesions may facilitate recruitment of TLS polymerase to the lesions that are difficult to be bypassed.

In **Aim 1**, we will determine whether ATR promotes TLS across 6-4PP lesions. This may explain why caffeine application immediately after UV prevents UV carcinogenesis, possibly due to blockage of error-prone TLS that occurs immediately after UV. This study will provide insight into how ATR inhibitors could be used to reduce the UV-induced mutation burden.

The role of ATR in TLS has not yet been elucidated. ATR inhibition reduces Pol eta recruitment to stalled replication forks after UV irradiation[43]. In yeast, the ATR-homolog Mec1 is important for the recruitment of Rev1 to damaged DNA and the formation of Pol zeta-Rev1 complex[44]. Rev1 is a DNA polymerase that does not incorporate nucleotides opposite UV lesions but is critical for recruiting Pol zeta to damaged DNA.

We hypothesize that mammalian ATR may regulate TLS activity of Pol zeta in a Rev1-dependent manner. No prior study has determined whether ATR regulates TLS across 6-4PP in human cells, thereby promoting mutagenesis. In **Aim 2**, we will determine whether ATR facilitates recruitment of Pol zeta to 6-4PP lesions (Figure 1.4).

Hypothesis:

ATR promotes cell survival but increases mutations by recruiting Pol zeta to UV lesions.

Aims:

Aim 1: To determine whether ATR is required for 6-4PP bypass.

Aim 2: To determine whether ATR facilitates the mutagenic bypass at 6-4PP lesions by recruiting Pol zeta to 6-4PP lesions.

These Specific Aims will improve our understanding of UV-induced mutagenesis by defining the role of ATR in error-prone TLS (6-4PP bypass). This study will help to develop novel strategies for suppressing UV mutagenesis by characterization of these poorly understood DNA damage tolerance mechanisms.

Figure 1.5 summarizes Specific Aims of this study that will address the mechanisms of UV-induced mutagenesis.

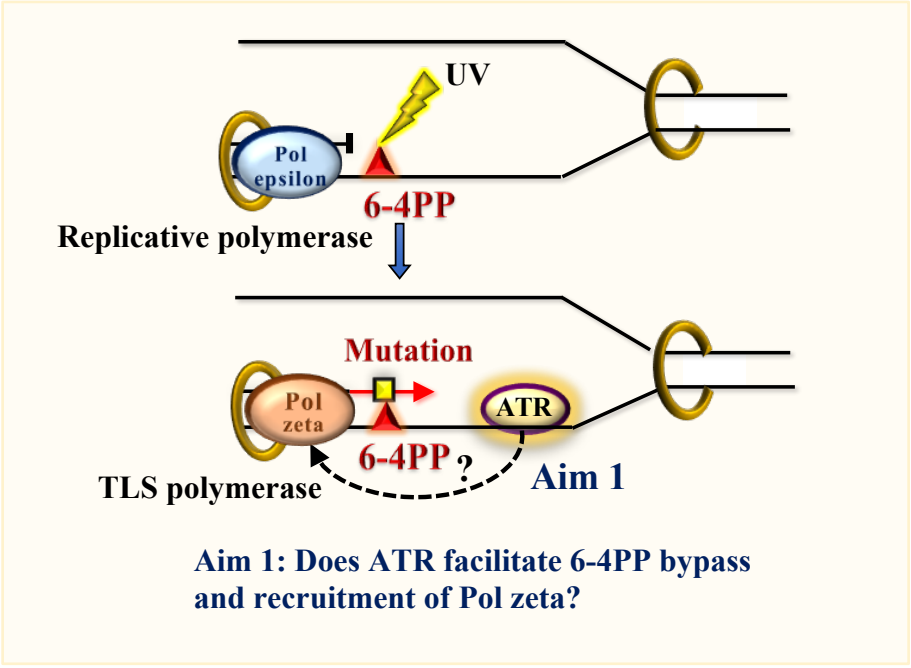

Figure 1.5. Overview of Specific Aims: Molecular mechanisms of error-prone DNA replication across UV lesions.

This study elucidates the mechanisms of UV mutagenesis at 6-4PP lesions. We will determine whether ATR promotes error-prone translesion synthesis (TLS) across 6-4PP lesions by recruiting Pol zeta (ζ) (Aim 1).

CHAPTER TWO: MATERIALS AND METHODS

2.1 Cell lines and culture conditions

Human XP-C fibroblast (defective NER pathway) cell lines with SV40-transformation (GM18983, XP4PA-SV-EB) were purchased from Coriell Cell Repositories (Camden, NJ). The cells were grown in Dulbecco's modified Eagle Medium (DMEM, #11995-040, Life Technologies) supplemented with 10% Fetal Bovine Serum (FBS; #10438-026, Life Technologies) and 1% Penicillin-Streptomycin (#15140-122, Life Technologies). XP-C cells were cultured at 37ºC in a humidified atmosphere of 5% CO2. Cells were harvested by trypsinization (incubated with trypsin at 37ºC for 5 minutes) using 0.05% Trypsin-EDTA (#25300, Life Technologies) for passage and harvest.

2.2 UV irradiation

Ultraviolet B (UV-B) irradiation was done by artificial light source using a panel of four UV-B bulbs (RPR- 3000, Southern New England Ultraviolet, Branford, CT) emitting radiation at 311 nm. Ultraviolet C (UVC) irradiation (<290 nm) was eliminated by use of a Kodacel filter (K6808, Eastman Kodak, Rochester, NY) covering the UV-B bulbs. The dose was monitored by a Photolight IL400A radiometer equipped with a SEL240/UV-B detector (International Light Technologies, Peabody, MA). 30 mJ/cm^2 of UV-B irradiation was used in all experiments and it typically required 45 sec. DMEM was aspirated and the cells were rinsed once with warm Hank's Balanced Salt Solution without phenol red (HBSS; #14025-092, Life Technologies). Once HBSS was aspirated, the dish containing cells was placed under UV-B light source without a lid until the dose reaches 30 mJ/cm^2. For sham-irradiated cells, the same treatment was used, without UV light.

2.3 Flow cytometry analysis of 6-4PP lesions

For experiments to determine the effect of ATR inhibitors in 6-4PP bypass, XP-C cells were plated on 35 mm dishes at a density of 0.5 x 10^6 cells per dish and incubated in DMEM medium for 16 h prior to UV irradiation. Two types of ATR chemical inhibitors were used in the study: caffeine (#C8960-250G, Sigma-Aldrich) and VE-821(#S8007, Selleckchem). Caffeine stock solution was prepared at 100 mM concentration with D-PBS (#14190-136, Invitrogen) by dissolving 0.194 g (MW 194.19) of caffeine powder in 10 ml of D-PBS at 37ºC. Caffeine solution in D-PBS was mixed with DMEM to give a final concentration of 3 mM concentration. For caffeine treatment, culture medium was replaced with DMEM containing caffeine at a concentration of 3 mM for 30 minutes prior to UV irradiation. For VE-821 treatment, the required amount of VE-821 (30 mM stock solution) was added to DMEM medium to achieve a final concentration of 10 μM. For VE-821 treatment, DMEM containing VE-821 (10 μM) was added to the cells 1 hour prior to UV irradiation. Following UV treatment, each dish is replaced with DMEM or DMEM containing caffeine or DMEM containing VE-821 and incubated at 37ºC until harvesting the cells.

The sham or UV treated cells were harvested by trypsinization at 0, 0.5, 1, 2 h after UV irradiation. Cell suspension was centrifuged at 200 x g for 5 min at 4ºC, and resuspended in 1 ml of ice-cold PBS. Cells were fixed by 2% formaldehyde by adding 143 μl of 16% paraformaldehyde (formaldehyde) aqueous solution (#15710, Electron Microscopy Sciences) to a 1 ml cell suspension in PBS. After adding formaldehyde, the cells were incubated at 37ºC for 10 min. Cells were then centrifuged at 700 x g for 5 min at 4ºC (these conditions were used for further centrifugation steps). The supernatant was aspirated and the pellet was resuspended in ice-cold 90% methanol and incubated at –20ºC overnight for permeabilization.

Cells were centrifuged next morning, and washed with 500 µl PBS before proceeding to DNase treatment. Cells that were sham irradiated or UV-treated, harvested at 0 h with or without ATR inhibitor, were treated with DNase. For DNase treatment, cells were centrifuged after the washing step, and the cell pellet was resuspended in 125 µl of 1x DNase reaction buffer containing 12.5 units of RQ1 RNase-free DNase (M6101, Promega) at 37ºC for 1 hr. After DNase treatment, cells were centrifuged and washed with 1 ml of bovine serum albumin (BSA; A9647, Sigma) in PBS. The blocking step was done by incubating cells in 200 µl of 1% BSA in PBS for 10 min at room temperature. For samples without DNase treatment, blocking was done after PBS wash step. Each sample was split into two aliquots, one half (equivalent to half of the cells from 35-mm dish) was centrifuged, and the pellet was resuspended in 100 µl of antibody dilution buffer (0.25% Tween-20-containing 1% BSA in PBS) containing the primary antibodies at the following dilutions: anti-6-4PP mouse monoclonal $IgG_{2a\kappa}$ (1:1000, clone 64M-2, CAC-NM-DND-002, Cosmo Bio), and anti-phospho-Chk1 (Ser345) (133D3) rabbit monoclonal (1:100, #2348, Cell Signaling Technology) antibodies. The samples were incubated at 4ºC overnight. Next, the cells were centrifuged and washed twice with 1 ml wash buffer (0.05% Tween-20-containing 1% BSA in PBS). Cells were resuspended in 100 µl of antibody dilution buffer containing the following secondary antibodies and incubated for 30 min at room temperature in the dark: Alexa Fluor 647-conjugated donkey anti-mouse IgG (H+L) (1:800, A31571, Life Technologies) for 6-4PP antibody and Alexa Fluor 488-conjugated goat anti-rabbit IgG (H+L) (1:200, A11034, Life Technologies) for pChk1 antibody. After secondary antibody incubation, cells were washed twice and resuspended in 200 µl of PBS containing 2 µg of propidium iodide (PI; P4170, Sigma) and 100 µg of RNase A (#19101, Qiagen). Cells were analyzed on a FACSCanto II Flow Cytometer (BD Biosciences), and the acquired data were analyzed using FlowJo. Fluorescence signals of phospho-

Chk1 and 6-4PP were measured in S phase cells that were defined as 2N < DNA content < 4N.

2.4 ATR knockdown by DsiRNA transfection

The dicer-substrate siRNAs (DsiRNAs) kit against human ATR was purchased from IDT (#DsiRNAhs.Ri.ATR.13, Integrated DNA technologies). A non-targeting DsiRNA [Control DsiRNA Negative Control (DS NC1, IDT)] was used as a non-specific control. Cells were transfected by lipofection using Lipofectamine RNAiMAX (#13778030). Three different concentrations were used for each DsiRNA (10 nM, 5 nM and 1 nM) and the combination of all three DsiRNAs was used at 10 nM concentration. Cells were plated in a 12-well plate (density 0.13 million) 16 h before transfection to get confluency of 60% to 70%. Before transfection, warm DMEM medium was added (0.9 ml) to each well of 12-well plate. Lipofectamine RNAiMAX (2.5 µl) was diluted in 50 µl reduced serum medium Opti-MEM. The required DsiRNA was diluted in Opti-MEM to 50 µl final volume. The diluted DsiRNA was added to the tube containing lipofectamine, mixed gently and incubated for 10 min at room temperature. The prepared complex was added to each well in drops and mixed gently by rocking the plate. Cells were harvested 48 h after transfection. Knockdown of ATR was analyzed by Western blot analysis.

2.5 Western blots

For pChk1 detection, cells were harvested by trypsinization 2 h after UV exposure and for ATR detection, 48 h after DsiRNA transfection. Cell suspensions were collected in 1.7-mL tubes and centrifuged at 450 × g for 5 min at 4 °C. Cell pellets were washed once in PBS and centrifuged again at 450 × g for 5 min at 4 °C. Cell pellets were resuspended in cell lysis buffer (1 x) (#9803, Cell Signaling Technology) supplemented with Complete Protease Inhibitor Cocktail (Roche

Applied Science) and PhosSTOP Phosphatase Inhibitor Cocktail (Roche Applied Science). After incubating on ice for 10 min, cell lysates were clarified by centrifugation at 22,000 × g for 5 min at 4 °C. Protein concentrations of cell lysates were determined by using the Bradford Protein Assay Dye Reagent (Bio-Rad Laboratories). Serial dilutions of BSA in cell lysis buffer were used for generating a standard curve in Bradford assay. Cell lysates containing equal amounts of total protein [10 μg for pChk1 detection and 15 μg for ATR detection] were mixed with NuPAGE LDS Sample Buffer (#NP 0007, Invitrogen) containing 2-mercaptoethanol and heated at 70°C for 10 min. Protein samples for pChk1 staining were separated in NuPAGE 10% Bis-Tris protein gel (#NP0303BOX, 1.0 mm, 15-well, Invitrogen) with MES running buffer (#NP0002, Invitrogen). For ATR detection, the protein samples were separated in 3-8% Tris-Acetate Gel (#EA03755BOX, 1.0 mm, 15-well, Invitrogen) with NuPAGE Tris-Acetate SDS Running Buffer (#LA0041, Invitrogen). Proteins were transferred to Immobilon-P PVDF Membrane (#IPSN07852, Millipore) using transfer buffer (#NP0006, Invitrogen). The molecular weight of pChk1 is 56 kDa, and See blue plus2 prestained protein standard (#LC5925, Novex) was used as marker (separation range: 3.5 kDa to 160 kDa). ATR has a predicted molecular weight of 315 kDa and HiMark prestained protein standard (#LC5699, Novex) was used as marker (separation range: 40 kDa to 500 kDa). For pChk1, blocking was done by incubating the membrane with 5% w/v non-fat dry milk in 1 x Tris-buffered saline containing 0.1% Tween 20 (TBST) for 1 h at room temperature. For ATR detection, blocking was done using 5% w/v BSA in 1x TBST, for 1 h at room temperature. The blot was incubated with antibodies against pChk1 [anti-phospho-Chk1 (Ser345) (133D3) rabbit monoclonal (1:1000, #2348, Cell Signaling Technology)] and ATR [1:200, ATR rabbit polyclonal antibody generated using a peptide spanning amino acids 1–20 of human ATR (Nghiem *et al.*, 2001)[34]] overnight at 4ºC. After 3 wash steps with 1x TBST (each for 1 min), the blot was

incubated with HRP conjugated donkey anti-rabbit (NA9340V) (1:5000, 1% non-fat dry milk in 1XTBST) for 1 h at room temperature. The blot was washed three times with 1 x TBST (15 min each). Chemiluminescent detection was done by adding 2 ml of ECL Western Blotting Detection Reagents (#RPN2209, GE Amersham) for 1 minute. Signals were exposed to Kodak BioMax XAR Film (Carestream Health).

2.6 Chromatin preparation

XP-C cells were UV-treated (30 mJ/cm^2) and harvested at various time points post-UV (4 h, 6 h, 8 h and 24 h). The harvested cells were rinsed with PBS and centrifuged. 200 µl of PBS containing 1% paraformaldehyde was added to the cell pellet, mixed by tapping and incubated at room temperature for 20 minutes. The sample was centrifuged at 4000 rpm (#5403, Eppendorf centrifuge) for 2 minutes. The supernatant was discarded and 200 µl of 125 mM Glycine was added to the pellet, briefly vortexed and incubated for 5 minutes at room temperature. The sample was centrifuged at 4000 rpm for 2 minutes. The supernatant was discarded and the pellet was rinsed with 200 µl of PBS. The sample was centrifuged again at 10000 rpm for 2 min and the pellet was resuspended in 100 µl of shearing buffer. The samples were then transferred to 0.5 ml Eppendorf tubes. The samples were then sheared in Bioruptor (ultrasound sound based shearing system) at 4^{0}C for three cycles of 15 minutes each. After shearing, the samples were centrifuged at 10000 rpm for 2 min, the supernatant was transferred to new tubes and stored at –80^{0}C until they are used in matrix-ChIP assay.

2.7 Matrix-chromatin immunoprecipitation (Matrix-ChIP) assay

We utilized a 96-well format for ChIP assays, known as matrix-ChIP assay. 96-well plate (#T-3060-1, GeneMate) for matrix-ChIP assay was prepared by incubating all wells overnight with 0.1 mg Protein A (# P7837, Sigma) in 50 ml PBS per well. The wells that are intended to be used are first rinsed by using PBS and later blocked by adding 100 µl blocking buffer [Blocking buffer: 5% BSA and 0.01% sheared salmon sperm DNA in immunoprecipitation (IP) buffer. IP buffer: 150 mM NaCl, 50 mM Tris-HCl (pH 7.5), 5 mM EDTA, NP-40 (0.5% vol/vol)] to each well. The plate was covered with parafilm and incubated with blocking buffer for 1 hour at room temperature on an orbital shaker (AROS 160, Thermolyne). While the plate is incubating with blocking buffer, 1.5 ml tube was prepared containing each antibody [Normal rabbit IgG (#2027, SCBT), Pol zeta-H220 (#48814, SCBT)] in blocking buffer at the desired concentration. A new 96-well plate was taken and labeled as 'preincubation plate'. Blocking buffer was added to the wells, followed by chromatin and diluted antibody. The plate was incubated for 1 hour in ultrasound water bath sonicator. The pre-incubated samples were transferred to the ChIP plate and incubated for 1 hour in the sonicator. After 1 hour, all the wells were washed with 100 µl ice-cold IP buffer followed by 100 µl ice-cold Tris-EDTA buffer (TE buffer: 10 mM Tris, 1 mM EDTA, pH 7.0) for three times each. After the wash step, 50 µl of elution buffer (25 mM Tris base, 1 mM EDTA, pH 10) with proteinase K enzyme (200 µg/ml) was added for eluting DNA from immunoprecipitated chromatin. After adding elution buffer, the plate was incubated for 45 min at 55ºC, followed by 10 min at 95-100ºC. Incubations were carried out in a Thermal Cycler. After the elution step, the DNA was used in quantitative polymerase chain reaction (qPCR) for analysis.

2.8 Quantitative polymerase chain reaction (qPCR)

First, qPCR primers were designed for Alu repeat regions. Primer sequences were as follows: forward primer- CGGTGGCTCACGCCTGTA, reverse primer- GAGTGCAGTGGCGCGATC. Next, the qPCR master mix was mixed with primer at a ratio of 1:20. 1 µl of primer with master mix was added to each well of 384-well plate followed by 1 µl of eluted DNA. For each sample, four replicates were used. The plate was agitated for mixing (2600 rpm, 15 sec) and spun down. The plate was then kept in a qPCR machine for amplification. The data was then analyzed.

CHAPTER THREE: RESULTS

Aim 1.1: Determine whether ATR is required for 6-4PP bypass

Determine the TLS activity at 6-4PP lesions by flow cytometry approach

For all our experiments, we used XP-C SV40-transformed fibroblasts (GM15983) that are deficient in nucleotide excision repair mechanism (the global genomic repair pathway). These cells retain the UV lesions for a longer time without DNA repair, allowing assessment of UV lesions by flow cytometry approach. We used an acute dose of 30 mJ/cm^2 UV-B in all our experiments, which is shown to be the lowest dose required to produce a high-enough number of 6-4PP lesions (~12 6-4PP and 55 CPD per 10^6 bases) for reproducible analysis[10].

A multiparameter flow cytometry approach was performed with two primary antibodies, anti-6-4PP antibody and anti-pChk1 antibody (to assess ATR activation) along with a DNA-binding dye (propidium iodide) for simultaneous detection of S phase cell cycle. Secondary antibodies conjugated with fluorophores were used against anti-pChk1 and anti-6-4PP antibodies for signal detection.

The TLS activity at 6-4PP lesions was assessed using an anti-6-4PP antibody that is lesion-specific. The binding of antibody to the lesion is generally blocked by double-strand DNA (dsDNA) (Figure 3.1). Only in the S phase when there is replication stalling leading to accumulation of single-stranded DNA (ssDNA) around the lesion[16], the anti-6-4PP antibody can bind to the lesion. If there is an increase in 6-4PP signal after UV, that would indicate the presence of unbypassed 6-4PP lesions surrounded by ssDNA.

An UV-irradiated sample harvested immediately after UV was treated with an enzyme DNase I, and was used as a positive control to measure all the lesions irrespective of replication stalling

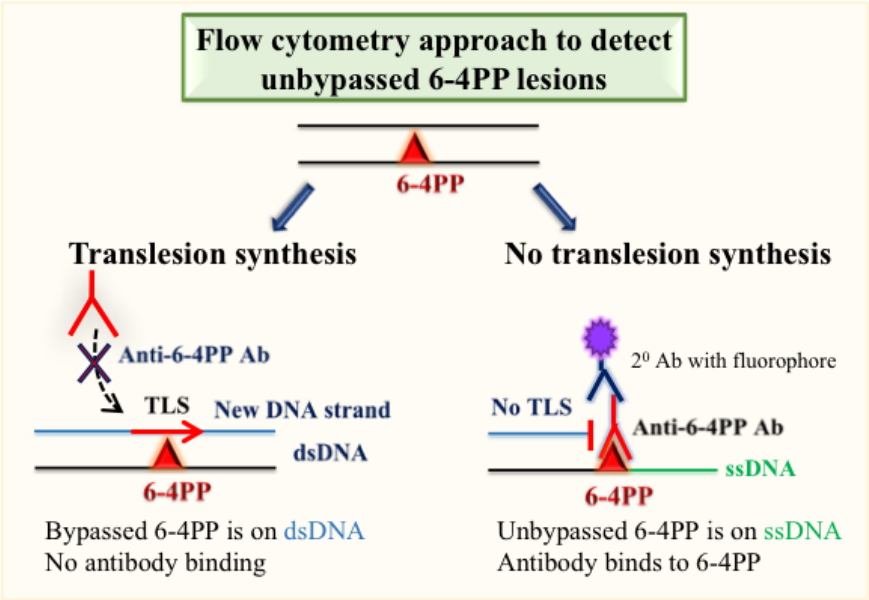

Figure 3.1. Detection of unbypassed 6-4PP lesions by lesion-specific antibody and flow cytometry.

Detection of 6-4PP lesions using antibody. 6-4PP antibody binds only to 6-4PPs that are on single-stranded DNA (ssDNA), but not on double-strand DNA (dsDNA). Unbypassed 6-4PPs caused by lack of TLS can be detected as increased signal in flow cytometry.

by the lesions. DNase I is an endonuclease, which causes single-stranded nicks leading to ssDNA, so that the antibody can bind to all the lesions in both strands of DNA. All the experimental samples were normalized to the positive control [UV 0 h, DNase (+)] and to the negative control [sham 0 h, DNase (+)].

To assess the base line of unbypassed UV lesions, XP-C cells harvested at various time points (0 h, 2 h, 4 h, 7 h) post-UV were stained with either anti-6-4PP [anti-6-4PP (64M-2)] or anti-CPD [anti-CPD (TDM-2)] antibody. Our results showed a slight increase in the CPD signal, but it remained at low levels at all post-UV time points that were analyzed (Figure 3.2 B). In contrast to this, 6-4PP signal increased significantly at all later time points compared to the sample harvested immediately after UV. This implies that 6-4PPs are the lesions that have ssDNA accumulation surrounding the lesion post-UV (Figure 3.2 A).

Determine the effect of ATR inhibition on 6-4PP bypass by using pharmacologic inhibition

To determine the effect of ATR on 6-4PP bypass, the cells were treated with ATR chemical inhibitors before and after UV treatment, and incubated with 6-4PP antibody after fixation. If ATR is critical for 6-4PP bypass, then the percentage of unbypassed 6-4PP signal are expected to increase when ATR is inhibited.

Two types of ATR inhibitors were used in our study: caffeine (non-specific ATR inhibitor) and VE-821 (specific ATR inhibitor). VE-821 is a potent and selective ATP competitive inhibitor of ATR.

Caffeine was used at a concentration of 3 mM with 30 min pre-incubation prior to UV, and was used at the same concentration post-UV until cell harvest. To determine the inhibitory concentration of VE-821, cells were incubated at various concentrations of VE-821 post-UV with

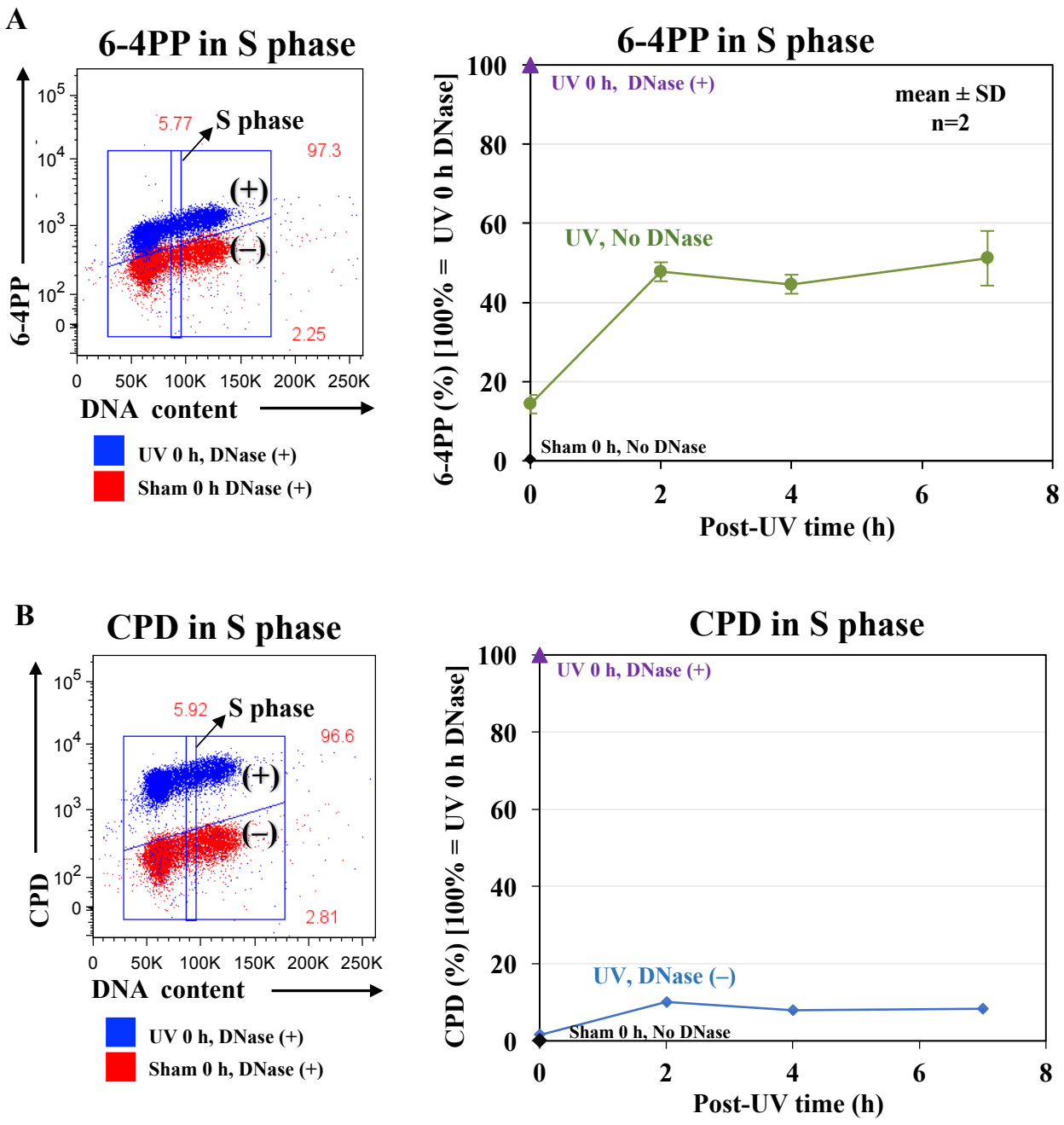

Figure 3.2. Detection of unbypassed UV lesions by lesion-specific antibody.

Flow cytometry approach using lesion specific antibody (anti-6-4PP and anti-CPD antibody) showed, unbypassed 6-4PP signal increased significantly in 2 h post-UV and continued to remain the same in later time-points (A). In contrast, unbypassed CPD signal did not increase significantly (B).

or without preincubation. Cells were harvested 2 h post-UV and protein lysates were prepared. Western blot was performed with pChk1 antibody to determine the effective inhibitory concentration of VE-821. The results showed that the signal intensity for pChk1 is weakest at 10 μM and 15 μM concentration of VE-821, indicating effective inhibition of ATR (Figure 3.3).

To characterize the effect of ATR inhibition, anti-pChk1 antibody was used along with 6-4PP antibody in flow cytometry. Chk1 phosphorylation (pChk1) is the key event following ATR activation by UV lesions[33]. pChk1 signal is expected to decrease in the presence of ATR inhibitors.

Nghiem et al. (2009)[35] have shown that pChk1 signal intensity is maximum at 1 h post-UV and the intensity decreases with time. To assess the effect of ATR inhibitor, cells were harvested at early time points (0 h, 0.5 h, 1 h, 2 h) after UV irradiation. The cells were treated with either VE-821 or caffeine and incubated with 6-4PP and pChk1 antibody.

The results showed more than 50% reduction in pChk1 signal at UV 1 h in VE-821-treated samples compared to samples without ATR inhibitor. Caffeine-treated samples showed only 30% reduction in pChk1 signal at UV 1 h, compared to samples without ATR inhibitor (Figure 3.4). 6-4PP signal increased significantly at UV 1 h and 2 h in samples treated with ATR inhibitors, compared to samples without ATR inhibitor. Experiments were repeated with VE-821 and the results were consistent with previous experiments showing an increase in unbypassed 6-4PP signal at 0.5 h, 1 h and 2 h post-UV (Figure 3.4). The observed increase in 6-4PP signal appeared to be similar in VE-821 or caffeine-treated samples.

Determine the effect of ATR inhibition on 6-4PP bypass by genetic inhibition via DsiRNA

To determine the effect of ATR inhibition on 6-4PP bypass by methods other than pharmacologic inhibition, genetic inhibition of ATR via DsiRNA was performed. ATR-specific

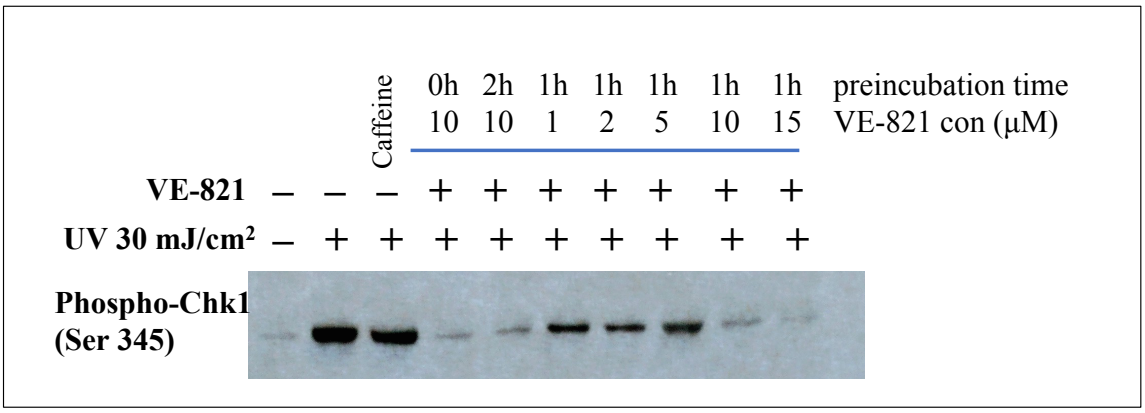

Figure 3.3. Determine the inhibitory concentration of VE-821 for XP-C cells.

XP-C cells were UV-treated and incubated with varying concentrations of VE-821 post-UV until harvest. pChk1 (downstream target of ATR) inhibition by VE-821 was detected by using anti-pChk1 antibody in western blot. VE-821 showed maximum inhibition at 10 μM and 15 μM concentration.

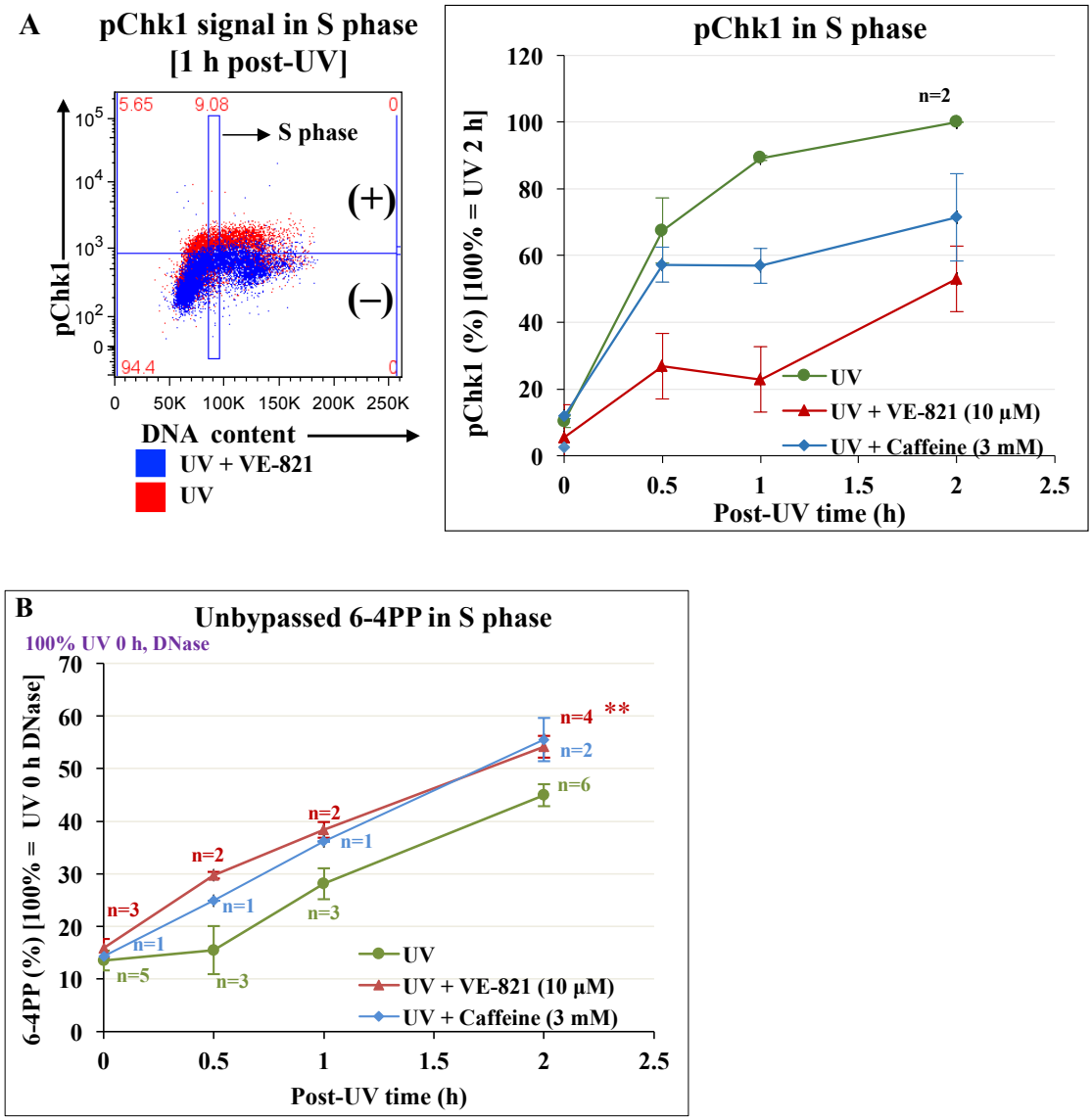

Figure 3.4. Determine the effect of ATR inhibitors in 6-4PP bypass.

The effect of ATR inhibition in 6-4PP bypass was determined by detecting unbypassed 6-4PP signal using flow cytometry approach. **(A)** ATR inhibition was analyzed by using pChk1 antibody in flow cytometry. pChk1 signal decrease significantly at 1 h post-UV in VE-821 or caffeine treated samples compared to UV alone samples. **(B)** UV-treated XP-C cells without ATR inhibitors showed significant increase in unbypassed 6-4PP signal at 2 h compared to 0 h. XP-C cells treated with caffeine or VE-821 showed marked increase in unbypassed 6-4PP signal at 1 h and 2 h post-UV compared to UV without ATR inhibitors. Results are mean ± SE, ** P value <0.05, Student's T-test.

dicer-substrate short interfering RNAs (DsiRNA from IDT) was used for ATR knockdown. Three different sequences of DsiRNA (DsiRNA-1, 2, 3) were tested at different concentrations and a combination of all three DsiRNAs was also tested. The results showed that DsiRNA-2 and combination of all 3 DsiRNAs gave maximum knockdown (~80% knockdown) compared to other sequences (Figure 3.5).

To determine the effect of genetic inhibition of ATR in 6-4PP bypass, XP-C cells treated with ATR DsiRNA were UV-treated and harvested at various time-points post-UV. The cells were stained with anti-6-4PP antibody and anti-pChk1antibody. The results showed that the unbypassed 6-4PP signal decrease at 2 h post-UV in cells treated with ATR-DsiRNA. ATR knockdown was indicated by decrease in pChk1 signal in ATR DsiRNA treated cells compared to the UV-treated control samples (Figure 3.6).

Aim 1.2: Determine whether ATR facilitate Pol zeta recruitment to 6-4PP lesions

Determine the role of ATR in Pol zeta recruitment to 6-4PP lesions by chromatin immunoprecipitation method

The chromatin immunoprecipitation assay (ChIP) is a powerful method to detect the recruitment of a protein of interest to chromatin. To determine whether ATR facilitates Pol zeta recruitment to 6-4PP lesions, a ChIP assay could be performed using anti-Pol zeta antibody with or without ATR inhibition. If ATR inhibition decreases Pol zeta recruitment to chromatin compared to control cells, then ATR is likely involved in recruitment of Pol zeta.

In this technique, cells are first treated with paraformaldehyde to covalently link a protein of interest to chromatin, and chromatin is then sheared mechanically. Specific antibodies against the

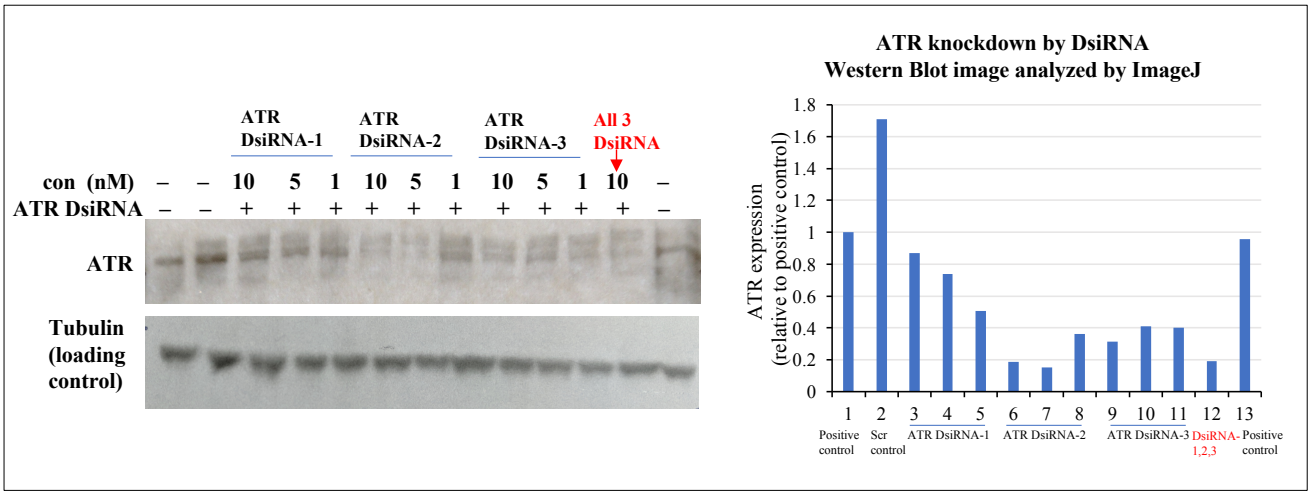

Figure 3.5. Optimization of ATR knockdown by DsiRNA.

XP-C cells were transfected with ATR DsiRNA for ATR knock-down. Three different sequences of DsiRNA were tested and they were used alone in different concentrations and in combination. Cells were harvested 48 h after transfection and analyzed by western blot using anti-ATR antibody. The combination of all three DsiRNA-1,2,3 and DsiRNA-2 at 10 nM concentration showed maximum knockdown compared to other samples.

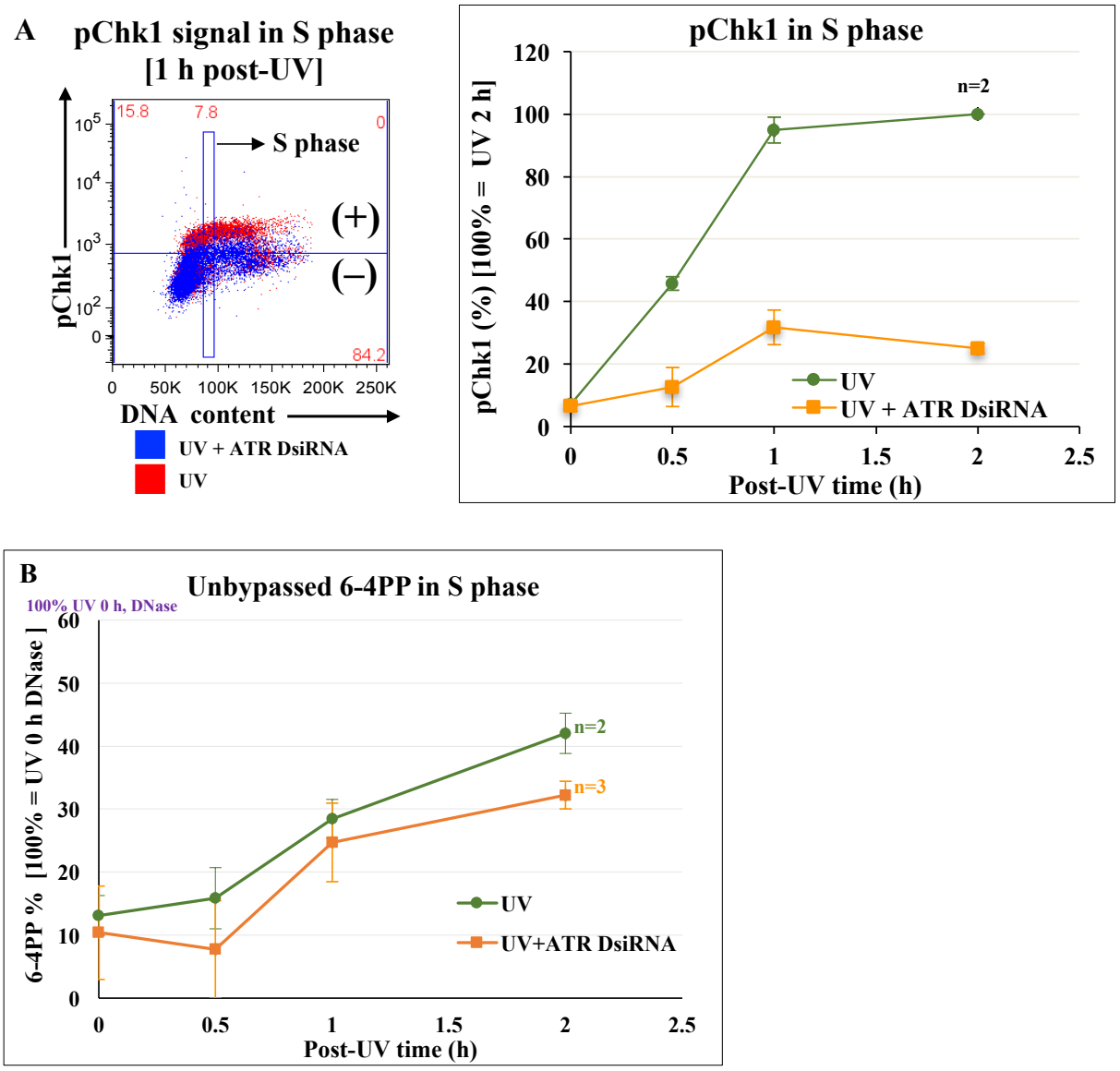

Figure 3.6. Determine the effect of ATR knockdown (by DsiRNA) in 6-4PP bypass by flow cytometry approach.

The effect of ATR inhibition by DsiRNA in 6-4PP bypass was determined by detecting unbypassed 6-4PP signal using flow cytometry approach. **(A)** ATR inhibition was analyzed by using pChk1 antibody in flow cytometry. pChk1 signal decrease in ATR DsiRNA treated samples compared to UV alone samples. **(B)** XP-C cells treated with ATR DsiRNA for ATR knockdown showed decrease in 6-4PP signal at 2 h post-UV compared to UV-treated cells without ATR inhibitors.

proteins of interest are used to enrich the cross-linked DNA–protein complexes, and this procedure is known as immunoprecipitation. The retrieved complexes are then analyzed by qPCR with gene-specific primers to quantify specific DNA targets[45,46].

XP-C (NER-deficient) cells are used to retain UV lesions that are normally repaired by NER. To specifically detect Pol zeta recruitment to 6-4PPs, double immunoprecipitation will be performed using two different antibodies: one against Pol zeta and the other against 6-4PP lesions (Figure 3.7). In the first step, Pol zeta-associated chromatin will be precipitated using Pol zeta antibody. After protein degradation and DNA denaturation, 6-4PP antibody will be used to precipitate 6-4PP-containing DNA.

ChIP assay normally involves amplification of specific gene locus to quantitate the amount of a specific DNA target to which a protein of interest is recruited. UV generates lesions on DNA randomly, and thus a specific gene locus may not contain DNA lesions following a moderate dose of UV. To overcome this problem, UV lesions are detected in Alu repeat regions. The Alu elements (~300 bp long) are repeat sequences with AluI restriction enzyme site and are present in ~1 million copies in the genome, comprising 10% of genome[47]. This approach is expected to increase the sensitivity of ChIP assay to detect UV lesions (Figure 3.7). Lesion-containing Alu repeats in the genome was quantitated by qPCR using Alu-specific primers. The amount of DNA detected by qPCR directly corresponds to Pol zeta recruitment to 6-4PP lesions.

Determine Pol zeta recruitment to UV-treated chromatin

XP-C cells were UV treated (30 mJ/cm^2) and harvested at various time points (2 h, 4 h, 6 h, 24 h) post-UV. The cells were then formalin fixed and chromatin shearing was carried out in a sonicator. The prepared chromatin was incubated with Pol zeta antibody (anti-Pol zeta antibody,

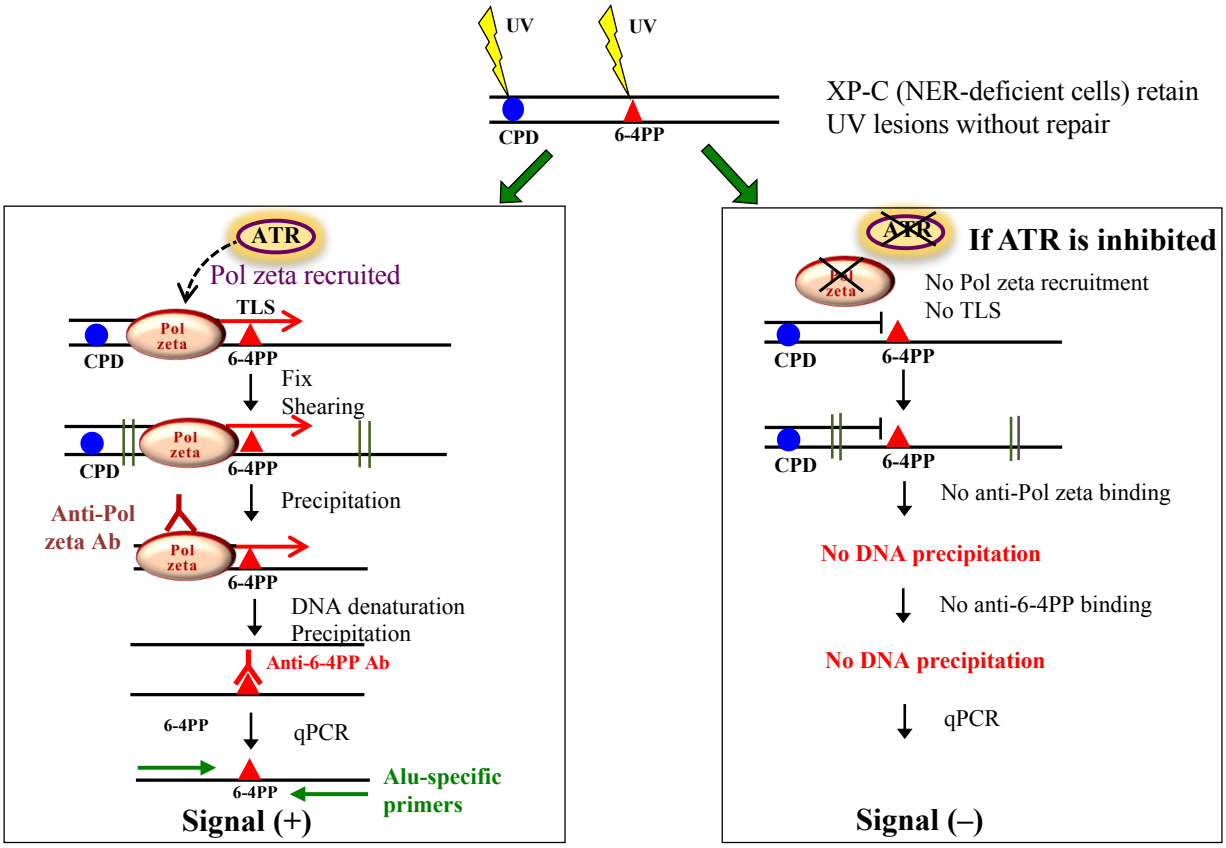

Figure 3.7. Double ChIP assay to detect Pol zeta recruitment specifically to 6-4PPs.

UV lesions will be generated in XP-C cells with or without ATR inhibitors. After fixing cells and shearing chromatin, immunoprecipitation will be performed with Pol zeta antibody. This will be followed by protein degradation and DNA denaturation to facilitate 6-4PP-antibody binding. Finally, the DNA will be amplified by qPCR using Alu-specific primers. Signal amplification by qPCR corresponds to Pol zeta recruitment to 6-4PPs. If ATR inhibitors decrease qPCR signal, it indicates that ATR is required for Pol zeta recruitment.

rabbit polyclonal) and immunoprecipitated in a protein A-coated 96-well plate. The DNA was then eluted from the immunoprecipitated chromatin and amplified by qPCR using Alu-specific primers.

The samples are normalized to input (without antibody) and the percentage of immunoprecipitated DNA was calculated for Alu-specific regions (Input%). Normal Rabbit IgG antibody was used as the negative control to determine baseline or non-specific immunoprecipitation. The samples incubated with Pol zeta are expected to have more immunoprecipitation than normal rabbit IgG.

The results showed that the ChIP signal (Input%) from Pol zeta is lower or equal to the ChIP signal (Input%) from normal IgG (Figure 3.8). This indicates that there was insufficient chromatin immunoprecipitation in samples immunoprecipitated by Pol zeta antibody.

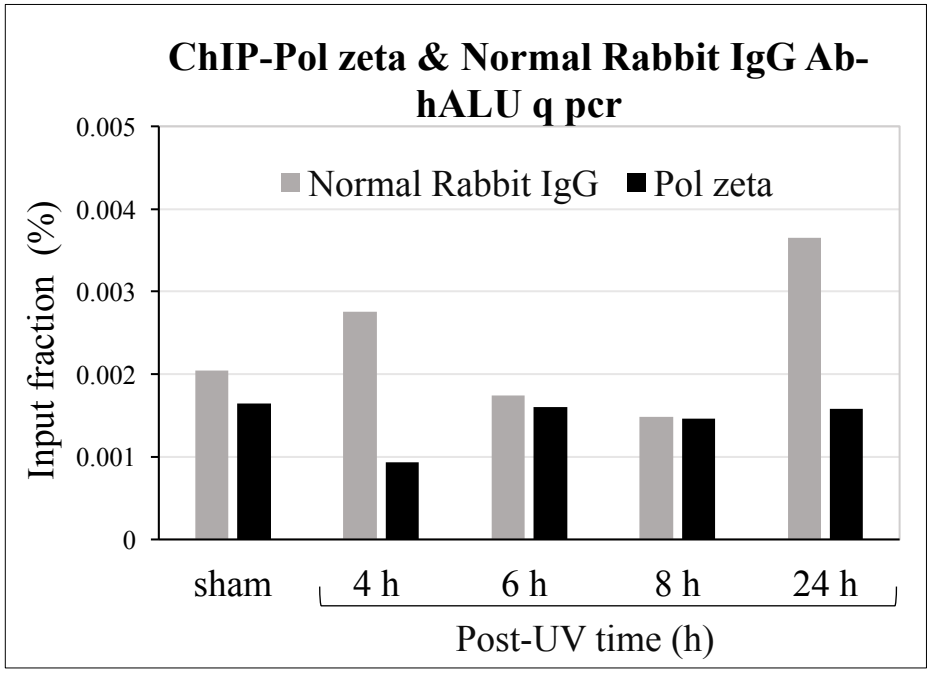

Figure 3.8. Determine Pol zeta recruitment to UV-treated chromatin by ChIP assay

XP-C cells were UV-treated and harvested at various time points post-UV. Chromatin samples prepared at the time of harvest and used in ChIP assay. ChIP assay using Pol zeta antibody did not show significant increase in ChIP signal compared to negative control normal rabbit IgG.

CHAPTER FOUR: DISCUSSION

The role of ATR in 6-4PP bypass

ATR inhibition by caffeine in UV-damaged cells showed augmented apoptosis which is a likely mechanism by which caffeine prevents skin cancer. However, there might be additional mechanisms underlying skin cancer prevention by ATR inhibition or caffeine.

We hypothesize that ATR inhibition immediately after UV radiation may block error-prone translesion synthesis. Importantly, we recently found that ATR is activated by 6-4PP lesions that are highly mutagenic, but not by CPD lesions (manuscript in revision). The significance of ATR activation at 6-4PP lesions has not been studied in detail. If ATR facilitates TLS activity at 6-4PP lesions, ATR inhibition might abrogate TLS activity, resulting in more unbypassed 6-4PP lesions (Figure 4.1).

The use of NER-deficient cells and lesion-specific antibody that can bind to 6-4PP allowed us to detect unbypassed 6-4PP lesions. Our multiparameter flow cytometry approach was advantageous for simultaneous assessment of ATR activation and unbypassed 6-4PP lesions. Our results showed that 6-4PP lesions remain unbypassed for a longer period compared to CPD lesions. It is possible that 6-4PP lesions are the ones that get surrounded by ssDNA, allowing antibody binding to the lesion and increased 6-4PP signal (Figure 3.2).

Conditional knockout or genetic inhibition of ATR (via DsiRNA) causes progressive loss of function which might preclude the analysis of immediate effects of ATR inhibition. To overcome this, we used a small molecule inhibitor (VE-821) that has high specificity for ATR kinase. It mimics the effects of ATR inhibition which was confirmed by decreased phosphorylation signal of the key downstream target of ATR (pChk1) (Figure 3.4). We analyzed the effect of VE-821 in

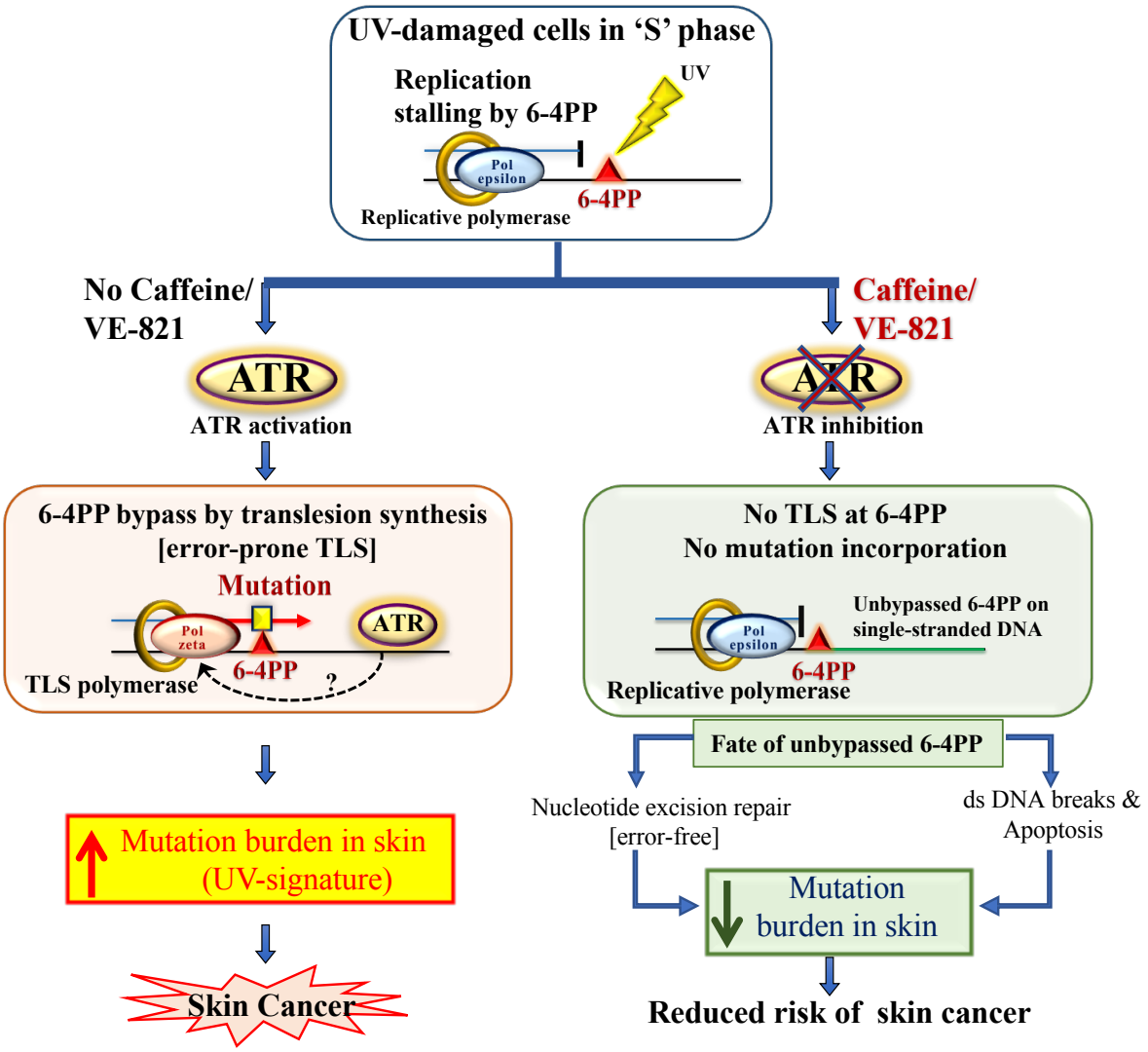

Figure 4.1. The role of ATR inhibitors in reducing UV- induced mutagenesis.

UV-damaged cells undergo replication stalling in S phase mainly at 6-4PP lesions leading to ATR activation. 6-4PP lesions are bypassed by translesion synthesis, that is potentially mutagenic. We hypothesize that ATR is important for this mutagenic TLS activity at 6-4PP lesions. We analyzed the effect of ATR treatment in 6-4PP bypass by measuring the unbypassed lesions using flow cytometry approach. Our results showed increased number of unbypassed 6-4PP lesions in cells treated with ATR inhibitors. The unbypassed 6-4PP lesions are expected to get repaired or become double stranded DNA breaks leading to apoptosis, thereby decreasing UV mutation burden.

6-4PP bypass. We also compared the effects of caffeine in 6-4PP bypass which is a non-specific inhibitor of ATR kinase[35].

Our results showed that there is an increase in unbypassed 6-4PP signal when ATR is inhibited by VE-821 or caffeine (Figure 3.4). The increase in unbypassed 6-4PP lesions surrounded by ssDNA after treatment with ATR inhibitors indicates that ATR activation is likely involved in 6-4PP bypass. The increased percentage of unbypassed 6-4PP lesions may be repaired at later time points or eventually turn into double-strand DNA breaks. Toledo et al (2013) showed that increased ssDNA leads to replication fork breakage through exhaustion of Replication Protein A (RPA)[48]. More unbypassed 6-4PP lesions surrounded by ssDNA may lead to increased double-strand breaks causing cell death. Thus, decreased TLS at 6-4PP lesions might potentially lead to reduced mutation incorporation (Figure 4.1).

We analyzed the effect of ATR inhibition by DsiRNA in 6-4PP bypass to assess whether pharmacologic inhibition of ATR has the same effect as genetic inhibition of ATR. Our results showed a decrease in the unbypassed 6-4PP signal at 2 hours in the ATR DsiRNA treated samples compared to samples without ATR DsiRNA treatment (Figure 3.6). The results from ATR DsiRNA inhibition are thus different from the results obtained from pharmacologic inhibition of ATR. The decrease in unbypassed 6-4PP signal in ATR DsiRNA inhibition might be due to premature replication fork collapse leading to double-strand DNA breaks, compared to pharmacologic inhibition of ATR.

The biology of replication fork stabilization might be different in different types of ATR inhibition. When ATR is inhibited by DsiRNA, ATR protein expression is decreased by ~80% and that is expected to decrease the formation of the ATR activation complex. In pharmacologic inhibition of ATR, there is competitive inhibition of kinase activity of ATR. The other functions

of ATR, mainly its ability to form complexes allowing the other assembled proteins to carry out their normal role, might be largely intact leading to replication fork stability for a longer period compared to ATR inhibition by DsiRNA. Other investigators [Chen et al, 2015] have also observed differences in ATR biology between pharmacologic and genetic inhibition. It has been reported that formation of double-strand DNA breaks after UV treatment increases when ATR is inhibited by siRNA compared to ATR inhibition by VE-821[49]. Chen et al used γH2AX as a marker for double-strand DNA breaks. This implies that the replication fork may collapse prematurely in ATR DsiRNA treated cells compared to VE-821 treated cells. The difference in γH2AX percentage in the two different methods of ATR inhibition (chemical inhibition vs genetic inhibition via siRNA) indicates that there could be differences in replication fork stability when ATR is inhibited by different methods.

Thus, decreased unbypassed 6-4PP signal could be due to increased double-strand breaks in ATR DsiRNA treated cells. However, additional experiments are needed to compare the expression of γH2AX with unbypassed 6-4PP signal in ATR DsiRNA treated samples and to understand if the mechanism of chemical inhibition of ATR is different from genetic inhibition by DsiRNA.

The role of ATR in Pol zeta recruitment to 6-4PP lesions

It is possible that ATR might be involved in recruitment of error-prone polymerase Pol zeta, and therefore ATR inhibition leads to decreased TLS activity at 6-4PP lesions. The ChIP experiment to determine Pol zeta recruitment to UV-treated chromatin in Alu-specific regions, did not show positive ChIP signal with Pol zeta antibody (Figure 3.8). The possible reasons are 1) the antibody (anti-Pol zeta) may not be suitable for ChIP assays, 2) the recruitment of Pol zeta could

be a transient event and this assay may not be sensitive enough to capture that event, 3) Alu-specific regions may not be ideal for assessing 6-4PP lesions.

To determine if Pol zeta antibody is the problem in the ChIP assay, a different antibody that is regularly used in ChIP assays could be used. For example, Pol zeta can be overexpressed using a plasmid containing a Flag epitope. An antibody against the Flag tag could then be used to detect Pol zeta recruitment to chromatin. DNA repeat regions other than Alu-specific regions may also be investigated for assessing 6-4PP lesions.

CHAPTER FIVE: SUMMARY AND FUTURE DIRECTIONS

Previous studies reported that the anti-cancer effect of ATR inhibition was partly due to increased UV-induced apoptosis. We analyzed the effect of ATR inhibition on 6-4PP bypass and showed that ATR is likely to facilitate an error-prone process which could potentially lead to an increased mutation frequency (Figure 4.1). This is of critical importance because UV mutagenesis can be controlled by ATR inhibition. The use of ATR-specific chemical inhibitors in sunscreens or post-UV lotions should be considered as a strategy to reduce UV carcinogenesis.

Further studies exploring the detailed molecular mechanisms would provide more insights into the UV mutagenesis process. ATR could be recruiting an error-prone polymerase (Pol zeta) that facilitates 6-4PP bypass. The ChIP approach for detecting Pol zeta recruitment could be optimized using a widely-used antibody such as anti-Flag antibody by overexpressing Pol zeta using a plasmid with a Flag tag. If ATR is facilitating Pol zeta recruitment, ATR inhibition is expected to decrease Pol zeta signal in UV-treated chromatin.

DNA sequencing to detect driver mutations could be used to determine if ATR inhibition decreases UV-induced mutagenesis. DNA from UV-treated cells with or without ATR inhibition could be compared to ascertain if cells with ATR inhibition have a reduced number of mutations. If the cells treated with ATR inhibitor showed fewer mutations, that would indicate ATR activation following UV irradiation is facilitating mutations of DNA.

BIBLIOGRAPHY

1. Rogers HW, Weinstock MA, Feldman SR, Coldiron BM. Incidence Estimate of Nonmelanoma Skin Cancer (Keratinocyte Carcinomas) in the U.S. Population, 2012. *JAMA Dermatol*. 2015;151(10):1081-6. PMID: 25928283.

2. Brash DE, Rudolph JA, Simon JA, Lin A, McKenna GJ, Baden HP, Halperin AJ, Ponten J. A role for sunlight in skin cancer: UV-induced p53 mutations in squamous cell carcinoma. *Proc Natl Acad Sci U S A*. 1991;88(22):10124-8. PMID: 1946433.

3. Runger TM. Role of UVA in the pathogenesis of melanoma and non-melanoma skin cancer. A short review. *Photodermatol Photoimmunol Photomed*. 1999;15(6):212-6. PMID: 10599968.

4. Pfeifer GP, You YH, Besaratinia A. Mutations induced by ultraviolet light. *Mutat Res*. 2005;571(1-2):19-31. PMID: 15748635.

5. de Gruijl FR, Sterenborg HJ, Forbes PD, Davies RE, Cole C, Kelfkens G, van Weelden H, Slaper H, van der Leun JC. Wavelength dependence of skin cancer induction by ultraviolet irradiation of albino hairless mice. *Cancer Res*. 1993;53(1):53-60. PMID: 8416751.

6. Rastogi RP, Richa, Kumar A, Tyagi MB, Sinha RP. Molecular mechanisms of ultraviolet radiation-induced DNA damage and repair. *J Nucleic Acids*. 2010;2010:592980. PMID: 21209706.

7. Kim JK, Patel D, Choi BS. Contrasting structural impacts induced by cis-syn cyclobutane dimer and (6-4) adduct in DNA duplex decamers: implication in mutagenesis and repair activity. *Photochem Photobiol*. 1995;62(1):44-50. PMID: 7638271.

8. Matsumura Y, Ananthaswamy HN. Toxic effects of ultraviolet radiation on the skin. *Toxicol Appl Pharmacol*. 2004;195(3):298-308. PMID: 15020192.

9. Perdiz D, Grof P, Mezzina M, Nikaido O, Moustacchi E, Sage E. Distribution and repair of bipyrimidine photoproducts in solar UV-irradiated mammalian cells. Possible role of Dewar photoproducts in solar mutagenesis. *J Biol Chem*. 2000;275(35):26732-42. PMID: 10827179.

10. Lo HL, Nakajima S, Ma L, Walter B, Yasui A, Ethell DW, Owen LB. Differential biologic effects of CPD and 6-4PP UV-induced DNA damage on the induction of apoptosis and cell-cycle arrest. *BMC Cancer*. 2005;5:135. PMID: 16236176.

11. de Lima-Bessa KM, Armelini MG, Chigancas V, Jacysyn JF, Amarante-Mendes GP, Sarasin A, Menck CF. CPDs and 6-4PPs play different roles in UV-induced cell death in normal and NER-deficient human cells. *DNA Repair (Amst)*. 2008;7(2):303-12. PMID: 18096446.

12. Marteijn JA, Lans H, Vermeulen W, Hoeijmakers JH. Understanding nucleotide excision repair and its roles in cancer and ageing. *Nat Rev Mol Cell Biol*. 2014;15(7):465-81. PMID: 24954209.

13. Moriwaki S. Human DNA repair disorders in dermatology: A historical perspective, current concepts and new insight. *J Dermatol Sci*. 2016;81(2):77-84. PMID: 26493104.

14. Kunkel TA. DNA replication fidelity. *J Biol Chem*. 2004;279(17):16895-8. PMID: 14988392.

15. Sale JE. Translesion DNA synthesis and mutagenesis in eukaryotes. *Cold Spring Harb Perspect Biol*. 2013;5(3):a012708. PMID: 23457261.

16. Jansen JG, Tsaalbi-Shtylik A, de Wind N. Roles of mutagenic translesion synthesis in mammalian genome stability, health and disease. *DNA Repair (Amst)*. 2015;29:56-64. PMID: 25655219.

17. Friedberg EC. Suffering in silence: the tolerance of DNA damage. *Nat Rev Mol Cell Biol*. 2005;6(12):943-53. PMID: 16341080.

18. Goodman MF. Error-prone repair DNA polymerases in prokaryotes and eukaryotes. *Annu Rev Biochem*. 2002;71:17-50. PMID: 12045089.

19. Lehmann AR. Replication of damaged DNA in mammalian cells: new solutions to an old problem. *Mutat Res*. 2002;509(1-2):23-34. PMID: 12427529.

20. Sale JE, Lehmann AR, Woodgate R. Y-family DNA polymerases and their role in tolerance of cellular DNA damage. *Nat Rev Mol Cell Biol*. 2012;13(3):141-52. PMID: 22358330.

21. Dieckman LM, Freudenthal BD, Washington MT. PCNA structure and function: insights from structures of PCNA complexes and post-translationally modified PCNA. *Subcell Biochem*. 2012;62:281-99. PMID: 22918591.

22. Friedberg EC, Lehmann AR, Fuchs RP. Trading places: how do DNA polymerases switch during translesion DNA synthesis? *Mol Cell*. 2005;18(5):499-505. PMID: 15916957.

23. McCulloch SD, Kunkel TA. The fidelity of DNA synthesis by eukaryotic replicative and translesion synthesis polymerases. *Cell Res*. 2008;18(1):148-61. PMID: 18166979.

24. Makarova AV, Burgers PM. Eukaryotic DNA polymerase zeta. *DNA Repair (Amst)*. 2015;29:47-55. PMID: 25737057.

25. Mouron S, Rodriguez-Acebes S, Martinez-Jimenez MI, Garcia-Gomez S, Chocron S, Blanco L, Mendez J. Repriming of DNA synthesis at stalled replication forks by human PrimPol. *Nat Struct Mol Biol*. 2013;20(12):1383-9. PMID: 24240614.

26. Chatterjee N, Walker GC. Mechanisms of DNA damage, repair, and mutagenesis. *Environ Mol Mutagen*. 2017;58(5):235-63. PMID: 28485537.

27. Lehmann AR. Translesion synthesis in mammalian cells. *Exp Cell Res*. 2006;312(14):2673-6. PMID: 16854411.

28. Gibbs PE, McDonald J, Woodgate R, Lawrence CW. The relative roles in vivo of Saccharomyces cerevisiae Pol eta, Pol zeta, Rev1 protein and Pol32 in the bypass and mutation induction of an abasic site, T-T (6-4) photoadduct and T-T cis-syn cyclobutane dimer. *Genetics*. 2005;169(2):575-82. PMID: 15520252.

29. Shachar S, Ziv O, Avkin S, Adar S, Wittschieben J, Reissner T, Chaney S, Friedberg EC, Wang Z, Carell T, Geacintov N, Livneh Z. Two-polymerase mechanisms dictate error-free and error-prone translesion DNA synthesis in mammals. *EMBO J*. 2009;28(4):383-93. PMID: 19153606.

30. Diaz M, Watson NB, Turkington G, Verkoczy LK, Klinman NR, McGregor WG. Decreased frequency and highly aberrant spectrum of ultraviolet-induced mutations in the hprt gene of mouse fibroblasts expressing antisense RNA to DNA polymerase zeta. *Mol Cancer Res*. 2003;1(11):836-47. PMID: 14517346.

31. Gan GN, Wittschieben JP, Wittschieben BO, Wood RD. DNA polymerase zeta (pol zeta) in higher eukaryotes. *Cell Res*. 2008;18(1):174-83. PMID: 18157155.

32. Lange SS, Bedford E, Reh S, Wittschieben JP, Carbajal S, Kusewitt DF, DiGiovanni J, Wood RD. Dual role for mammalian DNA polymerase zeta in maintaining genome stability and proliferative responses. *Proc Natl Acad Sci U S A*. 2013;110(8):E687-96. PMID: 23386725.

33. Cimprich KA, Cortez D. ATR: an essential regulator of genome integrity. *Nat Rev Mol Cell Biol*. 2008;9(8):616-27. PMID: 18594563.

34. Nghiem P, Park PK, Kim Y, Vaziri C, Schreiber SL. ATR inhibition selectively sensitizes G1 checkpoint-deficient cells to lethal premature chromatin condensation. *Proc Natl Acad Sci U S A*. 2001;98(16):9092-7. PMID: 11481475.

35. Heffernan TP, Kawasumi M, Blasina A, Anderes K, Conney AH, Nghiem P. ATR-Chk1 pathway inhibition promotes apoptosis after UV treatment in primary human keratinocytes: potential basis for the UV protective effects of caffeine. *J Invest Dermatol*. 2009;129(7):1805-15. PMID: 19242509.

36. Kawasumi M, Lemos B, Bradner JE, Thibodeau R, Kim YS, Schmidt M, Higgins E, Koo SW, Angle-Zahn A, Chen A, Levine D, Nguyen L, Heffernan TP, Longo I, Mandinova A, Lu YP, Conney AH, Nghiem P. Protection from UV-induced skin carcinogenesis by genetic inhibition of the ataxia telangiectasia and Rad3-related (ATR) kinase. *Proc Natl Acad Sci U S A*. 2011;108(33):13716-21. PMID: 21844338.

37. Abel EL, Hendrix SO, McNeeley SG, Johnson KC, Rosenberg CA, Mossavar-Rahmani Y, Vitolins M, Kruger M. Daily coffee consumption and prevalence of nonmelanoma skin cancer in Caucasian women. *Eur J Cancer Prev*. 2007;16(5):446-52. PMID: 17923816.

38. Ferrucci LM, Cartmel B, Molinaro AM, Leffell DJ, Bale AE, Mayne ST. Tea, coffee, and caffeine and early-onset basal cell carcinoma in a case-control study. *Eur J Cancer Prev*. 2014;23(4):296-302. PMID: 24841641.

39. Loftfield E, Freedman ND, Graubard BI, Hollenbeck AR, Shebl FM, Mayne ST, Sinha R. Coffee drinking and cutaneous melanoma risk in the NIH-AARP diet and health study. *J Natl Cancer Inst*. 2015;107(2). PMID: 25604135.

40. Naganuma T, Kuriyama S, Kakizaki M, Sone T, Nakaya N, Ohmori-Matsuda K, Nishino Y, Fukao A, Tsuji I. Coffee consumption and the risk of oral, pharyngeal, and esophageal cancers in Japan: the Miyagi Cohort Study. *Am J Epidemiol*. 2008;168(12):1425-32. PMID: 18974083.

41. Galeone C, Tavani A, Pelucchi C, Turati F, Winn DM, Levi F, Yu GP, Morgenstern H, Kelsey K, Dal Maso L, Purdue MP, McClean M, Talamini R, Hayes RB, Franceschi S, Schantz S, Zhang ZF, Ferro G, Chuang SC, Boffetta P, La Vecchia C, Hashibe M. Coffee and tea intake and risk of head and neck cancer: pooled analysis in the international head and neck cancer epidemiology consortium. *Cancer Epidemiol Biomarkers Prev*. 2010;19(7):1723-36. PMID: 20570908.

42. Sarkaria JN, Busby EC, Tibbetts RS, Roos P, Taya Y, Karnitz LM, Abraham RT. Inhibition of ATM and ATR kinase activities by the radiosensitizing agent, caffeine. *Cancer Res*. 1999;59(17):4375-82. PMID: 10485486.

43. Chen YW, Cleaver JE, Hatahet Z, Honkanen RE, Chang JY, Yen Y, Chou KM. Human DNA polymerase eta activity and translocation is regulated by phosphorylation. *Proc Natl Acad Sci U S A*. 2008;105(43):16578-83. PMID: 18946034.

44. Hirano Y, Sugimoto K. ATR homolog Mec1 controls association of DNA polymerase zeta-Rev1 complex with regions near a double-strand break. *Curr Biol*. 2006;16(6):586-90. PMID: 16546083.

45. Gade P, Kalvakolanu DV. Chromatin immunoprecipitation assay as a tool for analyzing transcription factor activity. *Methods Mol Biol*. 2012;809:85-104. PMID: 22113270.

46. Schoppee Bortz PD, Wamhoff BR. Chromatin immunoprecipitation (ChIP): revisiting the efficacy of sample preparation, sonication, quantification of sheared DNA, and analysis via PCR. *PLoS One*. 2011;6(10):e26015. PMID: 22046253.

47. Batzer MA, Deininger PL. Alu repeats and human genomic diversity. *Nat Rev Genet*. 2002;3(5):370-9. PMID: 11988762.

48. Toledo LI, Altmeyer M, Rask MB, Lukas C, Larsen DH, Povlsen LK, Bekker-Jensen S, Mailand N, Bartek J, Lukas J. ATR prohibits replication catastrophe by preventing global exhaustion of RPA. *Cell*. 2013;155(5):1088-103. PMID: 24267891.

49. Chen T, Middleton FK, Falcon S, Reaper PM, Pollard JR, Curtin NJ. Development of pharmacodynamic biomarkers for ATR inhibitors. *Mol Oncol*. 2015;9(2):463-72. PMID: 25459351.

ACKNOWLEDGMENTS

Firstly, I would like to thank **Dr. Richard Presland** for helping me to select a lab for my thesis work. I am highly grateful for his amazing support and contribution throughout my course.

I would like to thank my thesis committee for their guidance with my training at the University of Washington. I would like to thank my mentor **Dr. Paul Nghiem** for giving me this opportunity to work in his lab. His invaluable support and advice about science, career and life during made me stronger in every possible way. I would also like to thank my co-supervisor **Dr. Masaoki Kawasumi** for sharing his knowledge and for playing a major role in improving my scientific skills. I would like to thank **Dr. Karol Bomzstyk** for his valuable scientific advice and generous support in helping me to learn a new technique (ChIP assay).

I would like to thank the past and present members of the **Ngheim Lab**, **Kawasumi Lab**, and **Bomzstyk lab**. I am grateful to receive their generous offer with training/assistance/knowledge.

I want to thank my whole family, especially my parents and my husband who always support me, believe in me, and love me.